DE LA RECHERCHE À L'INDUSTRIE

INSPYRE end of spring school

Fast reactor fuel microstructure and thermal performance
+
Post irradiation examinations

J. Noirot

May 2019

www.cea.fr

Reactors, and Hot Cell Laboratories

- Irradiations
- Instrumented irradiations
- Post irradiation examinations
- Tests in test reactors
- Tests in hot cell

- Non irradiated experiments
- Theoretical work, Modelling

} Fuel behavior understanding

The beauty of fuel behavior modelling

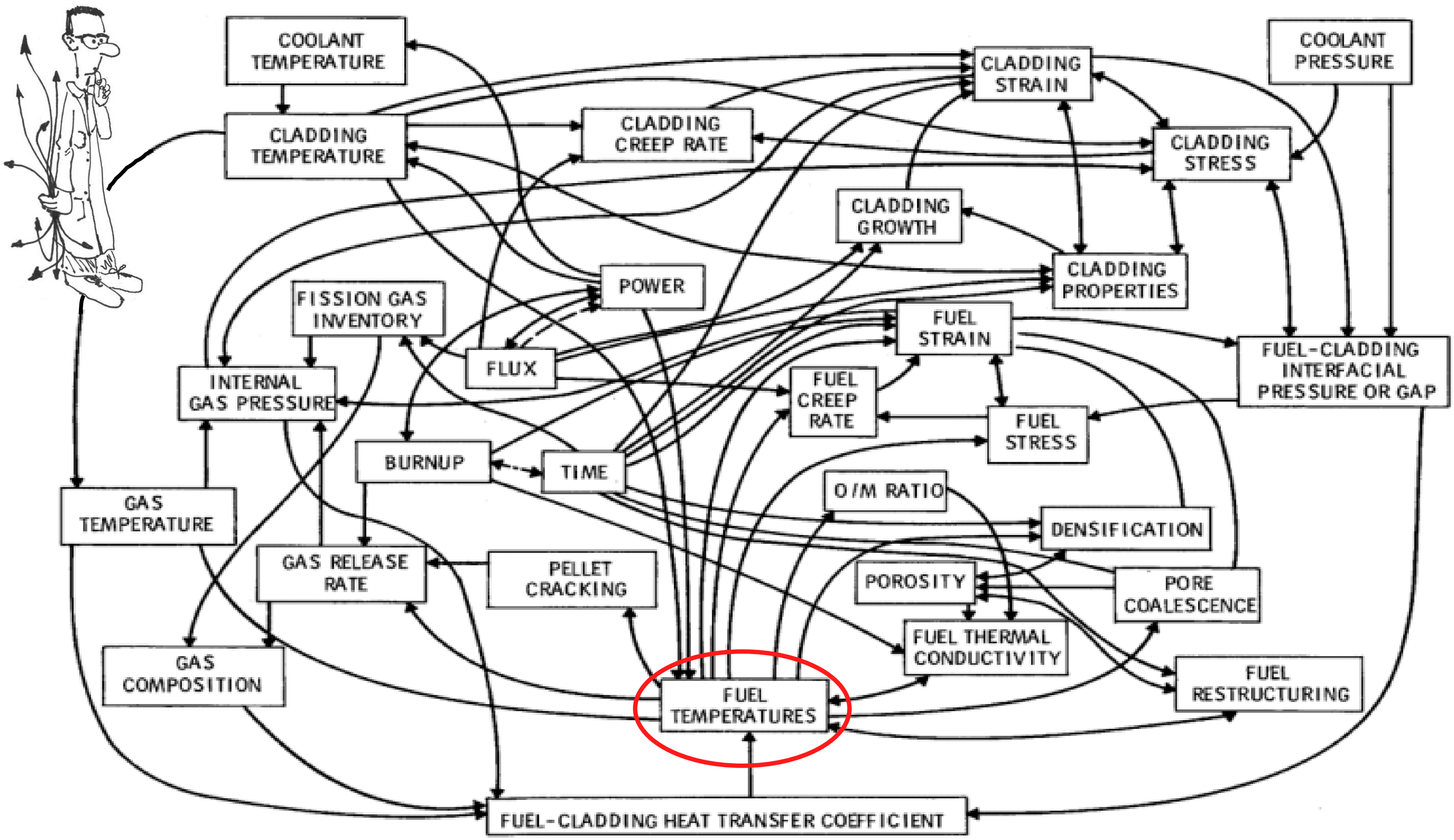

C . E. **Beyer**, C . R. Hann, D. D. Lanning, F. E. Panisko, and L. J. Parchen
Report t o Core Performance Branch Division of Technical Review Nuclear Regulatory Commission November 1975
BATTELLE PACIFIC NORTHWEST LABORATORIES
(maybe Horn G.P. 1973)

Fuel temperatures

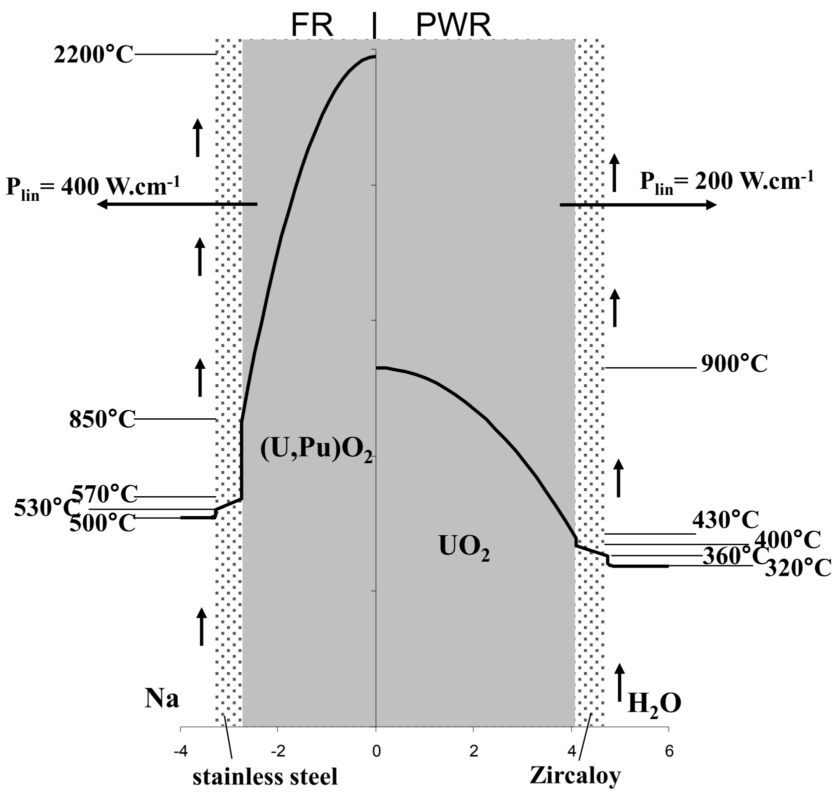

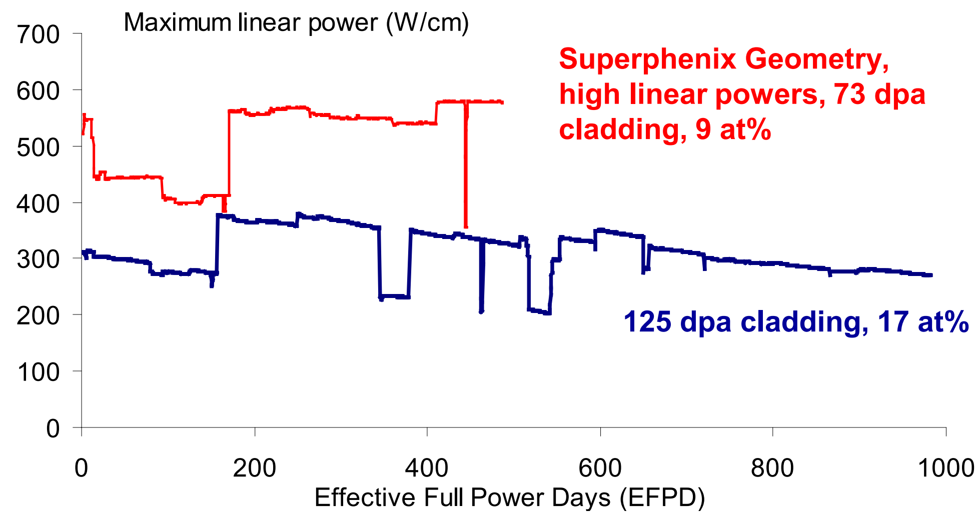

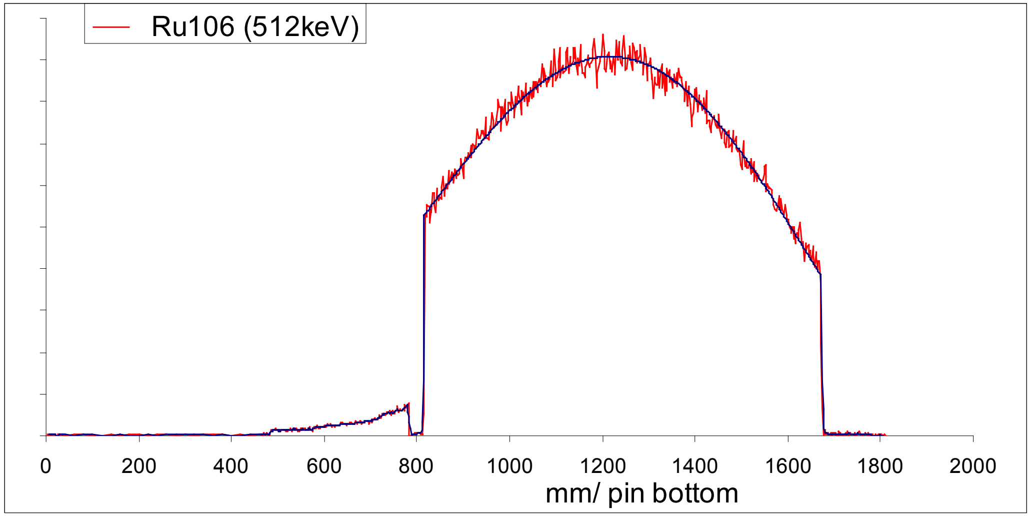

- Generally higher temperatures in FR fuels / LWR fuels
- Not all fuels see the same temperatures
- Temperature changes with time
- Not the same temperature everywhere in a pin

Thermal conductivity and melting temperature

- UO_2 and $(U,Pu)O_2$ → rather poor thermal conductivity

Pu/(U+Pu) = 0.2	Carbide (U,Pu)C	Nitride (U,Pu)N	Oxide $(U,Pu)O_2$	Metallic fuel (U,Pu,Zr)
Heavy atom density (g/cm^3)	12.95 (+ 33 %)	13.53	9.75	14
Melting point (°C)	2420	2780	2750	1080
Thermal conductivity ($W.m^{-1}.K^{-1}$)	16.5	14.3	2.9	14

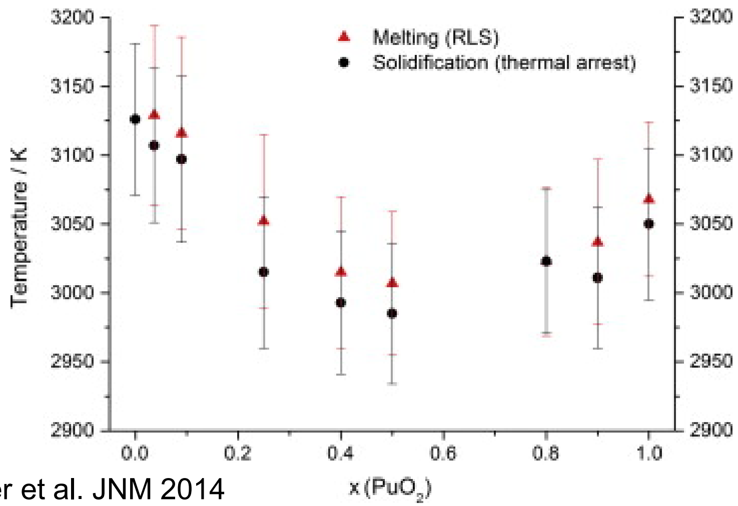

Bölher et al. JNM 2014

Laser heating and fast pyrometry

reflected Light Signal technique,
→ avoids interactions with the crucible

Thermal conductivity

- Thermal diffusivity: laser flash

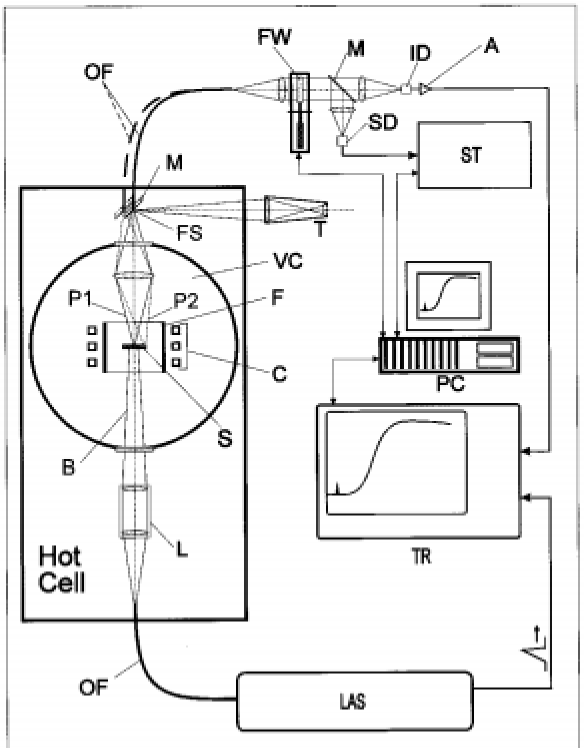

FIG. 1. Schematic of the LAF-1 laser flash system. LAS, probe laser; OF, optical fiber; L, lenses; B, focused laser beam; S, sample; C, HF heating coil; P1 and P2, variable observed surface areas; VC, vacuum vessel; M, movable mirror; T, telescope; FW, pyrometer optical filters; ID, InGaAs photodiode; A, amplifier; SD, pyrometer Si photodiode; ST, steady-state pyrometer electronics; PC, computer; and TR, transient recorder.

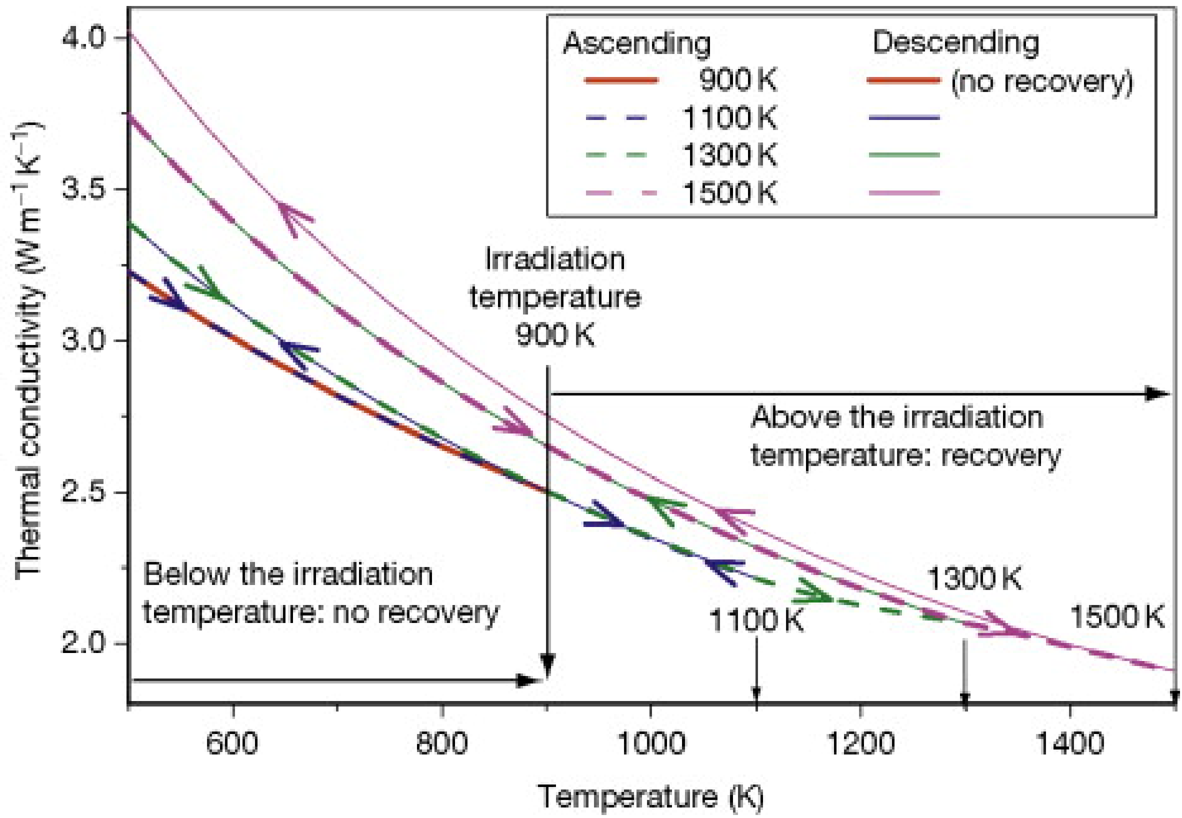

Staicu 2012

M. Sheindlin et al. Review of scientific instruments 1998

Thermal conductivity

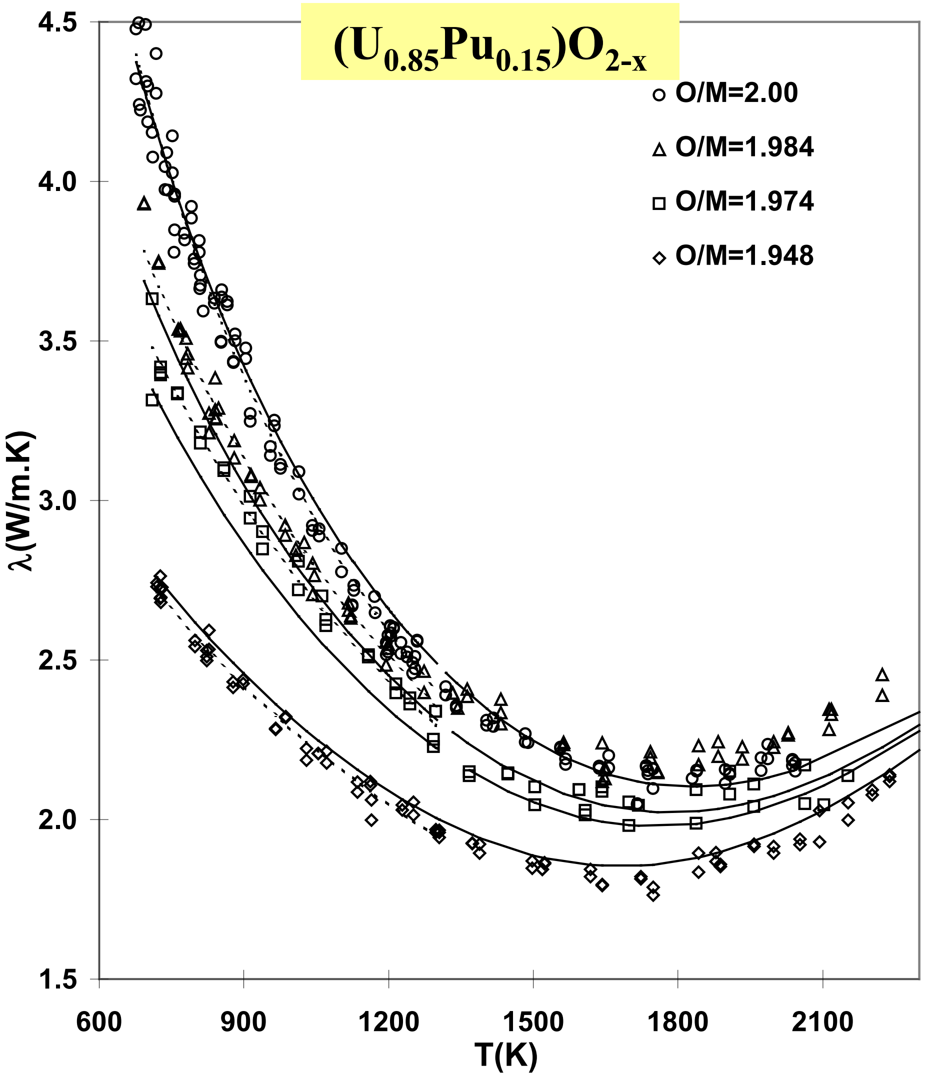

Duriez 2000

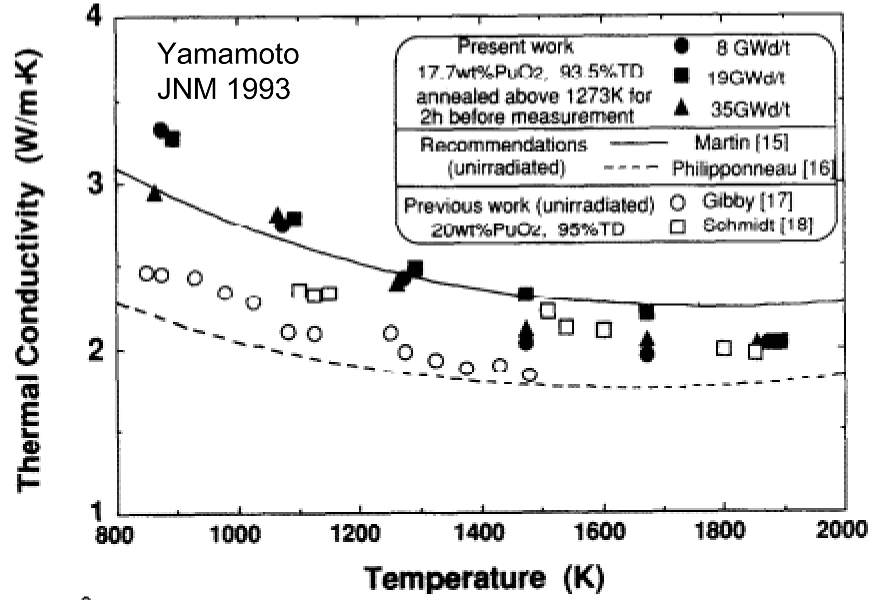

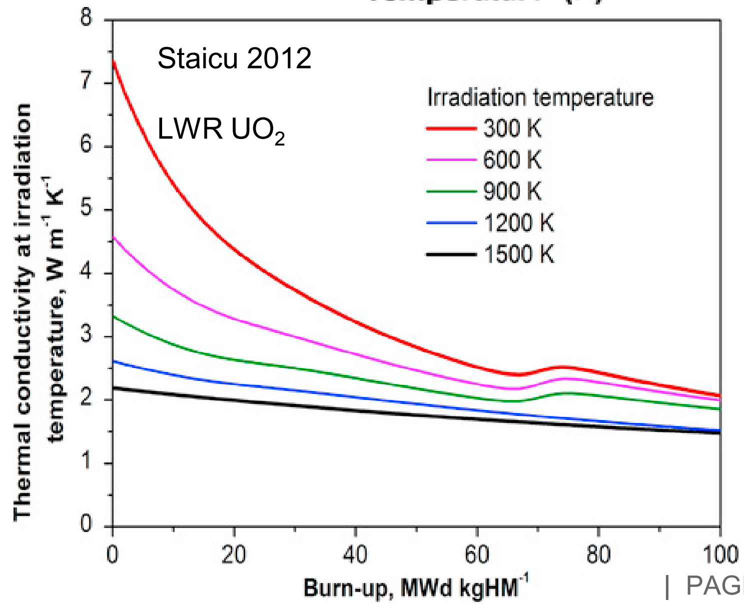

Cladding strain, visual examinations, Diameter measurements

- Very high fluences~ 10^{27} n/cm² # 150 dpa
- Steel swelling

helicoïdal pins ΔV/V cladding> wire

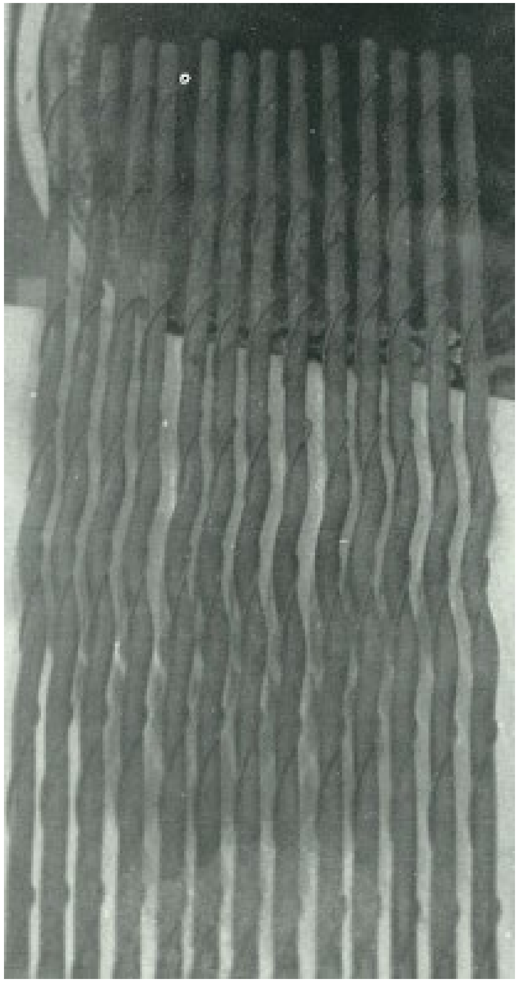

wire displacement ΔV/V wire> cladding

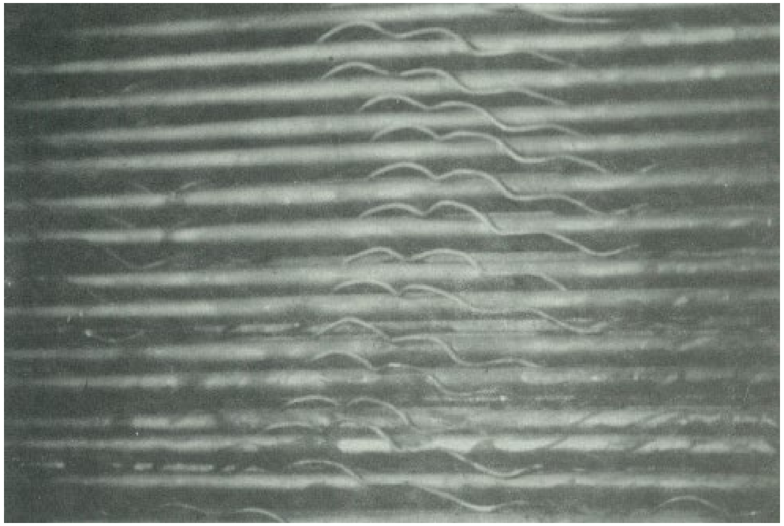

Interactions between pins
➔ ovalizations
➔ contacts

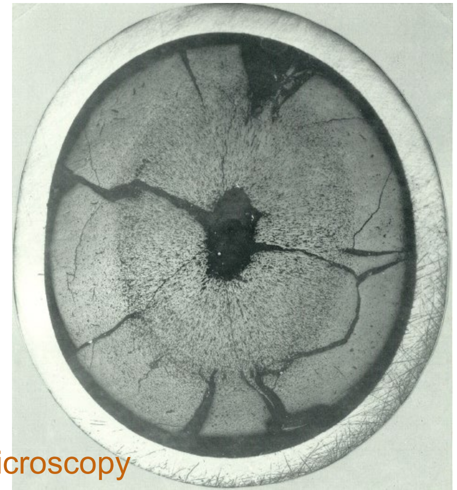

Optical microscopy

- Steel improvements

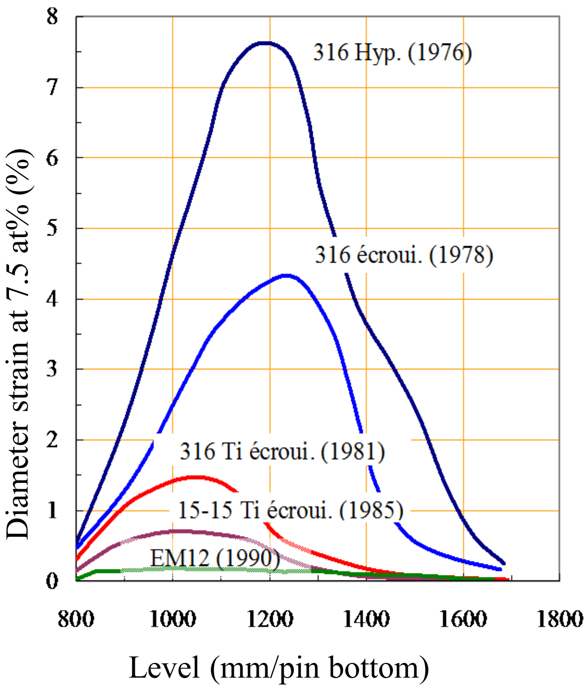

Diameter measurements

X-ray radiography

- Minoru YONEKAWA et al. JAEA review 2010-049

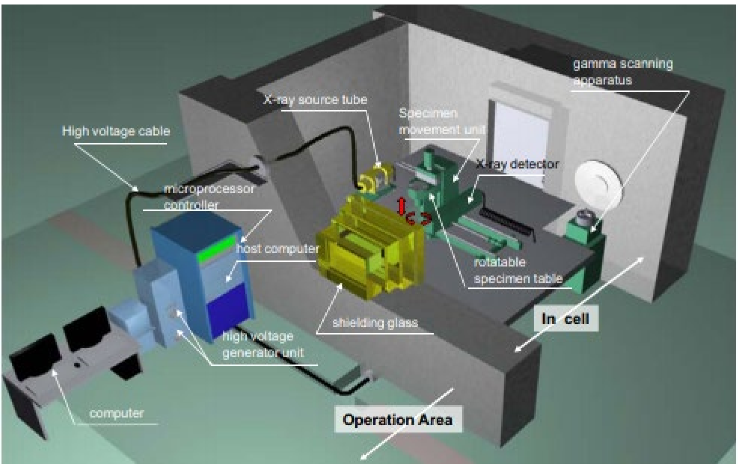

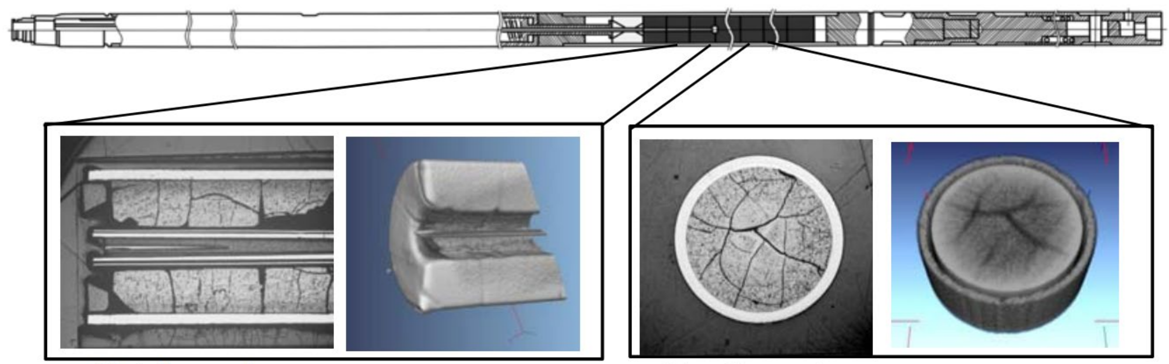

Metallography (Longitudinal section) | tomography | Metallography (cross-section) | tomography

First generation X-ray method | Second generation X-ray method | Third generation X-ray method

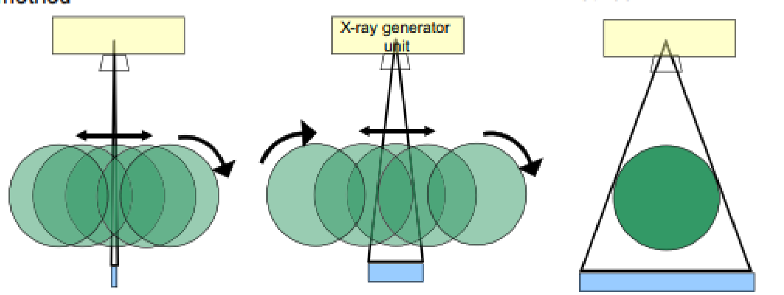

X-ray detector unit :1 piece | X-ray detector unit :some100 piece | X-ray detector unit :more than2000piece

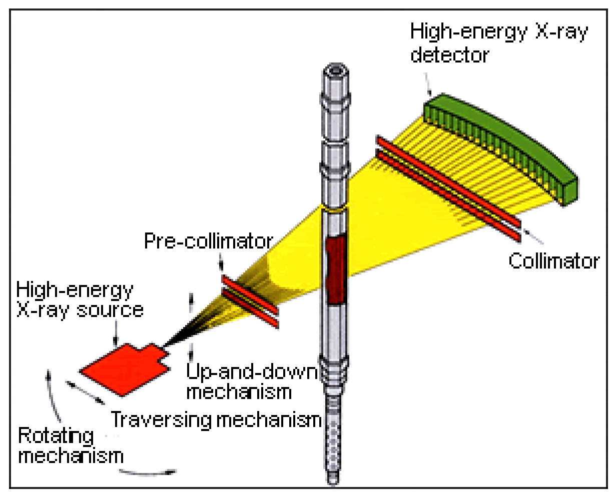

Principle of the Imaging

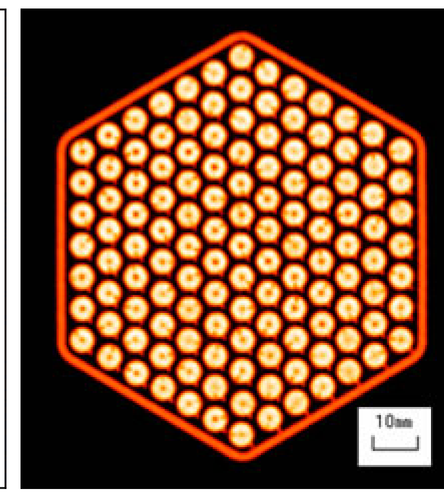

Cross-section Image of Driver Fuel Subassembly

X-ray radiography

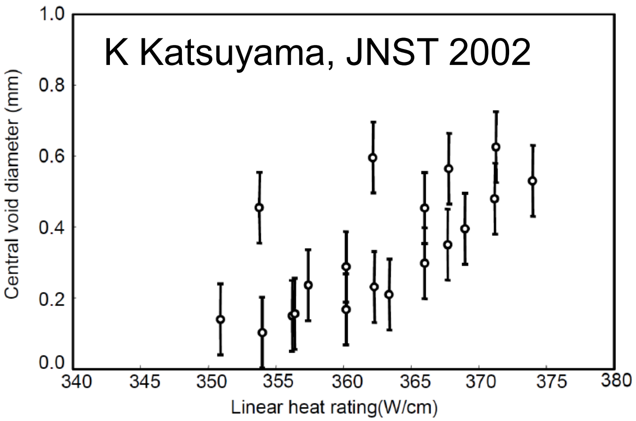

A. Ishimi, JNST 2012

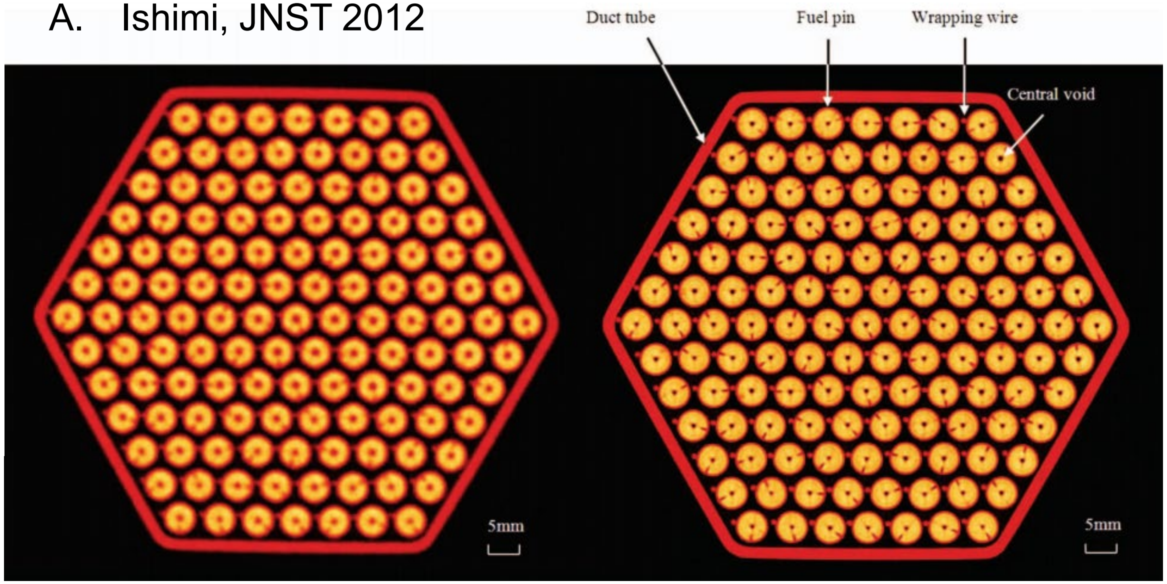

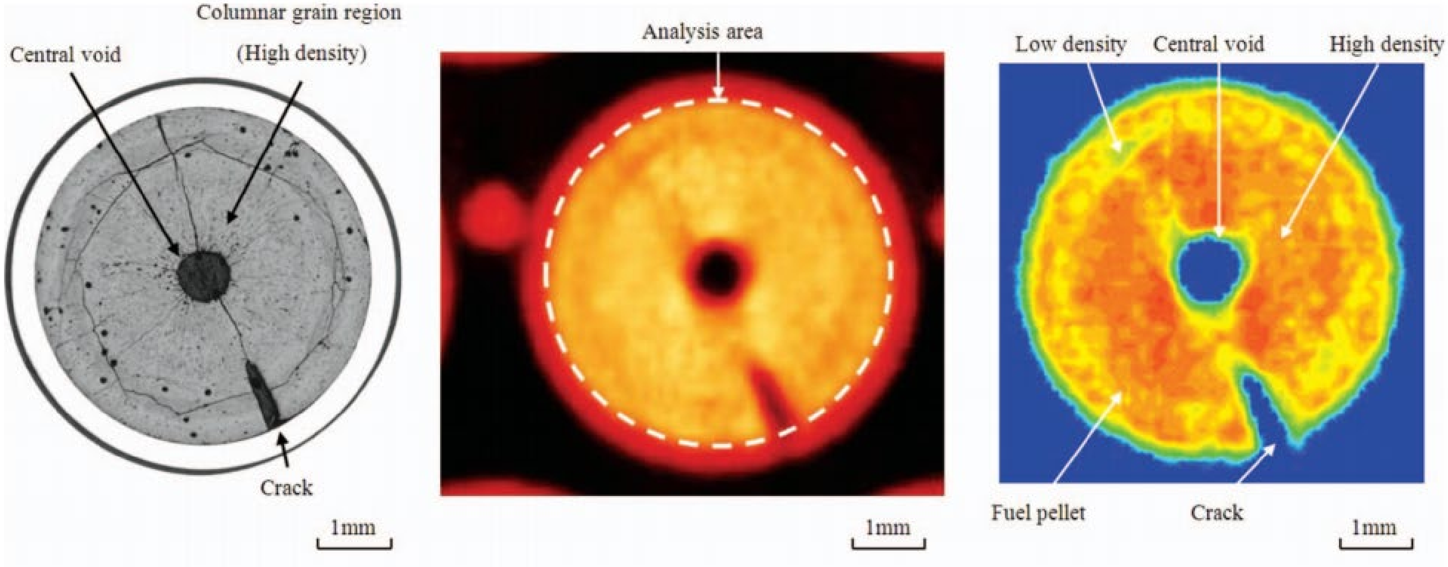

Non Destructive Examinations: Gammascanning, Diameter measurements, Eddy currents

- Diameter measurement

Contact between the pin and WC knifes + LVDT (Linear Variable Differential Transformer).

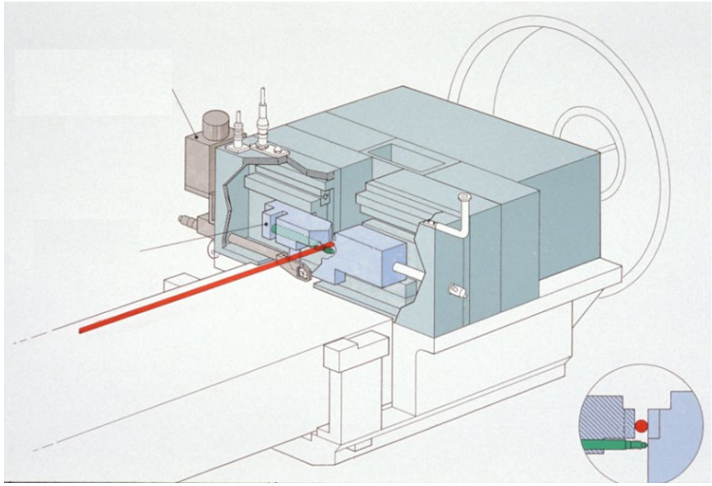

- Eddy currents

Alternative currents in coils around the pin, Eddy currents induced in the metallic cladding. Impedance in the coils sensitive to defects in the cladding .

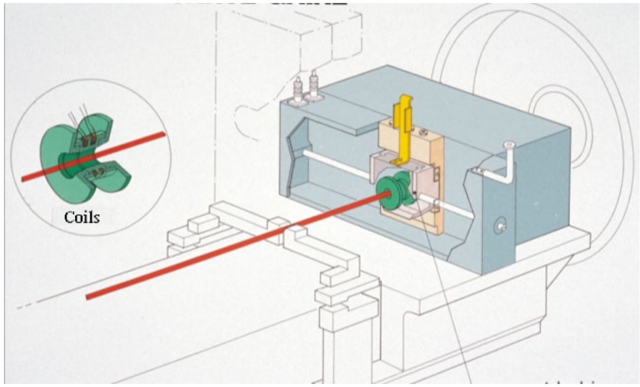

- gammascanning → axial distribution of gamma emitting isotopes

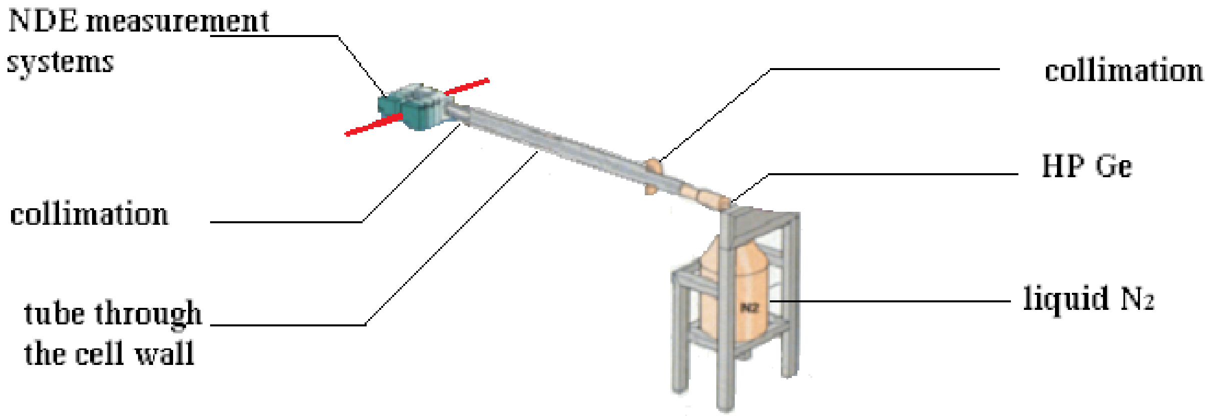

Non Destructive Examinations: Gammascanning, Diameter measurements, Eddy currents

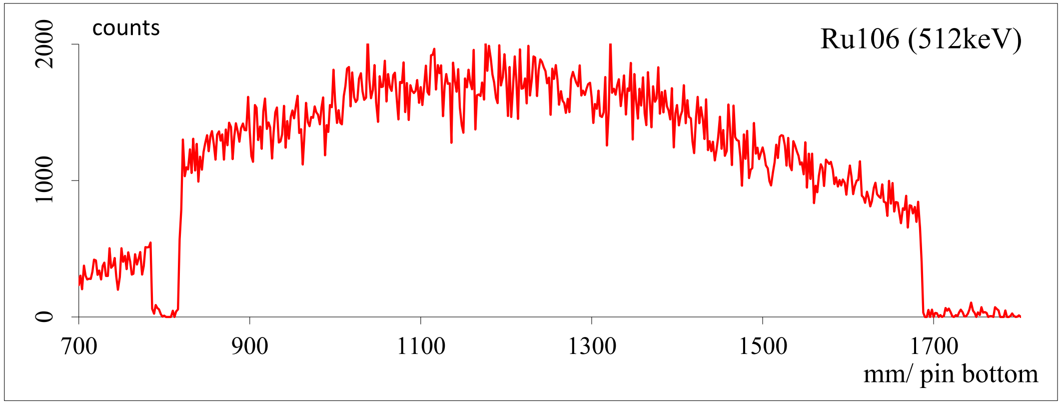

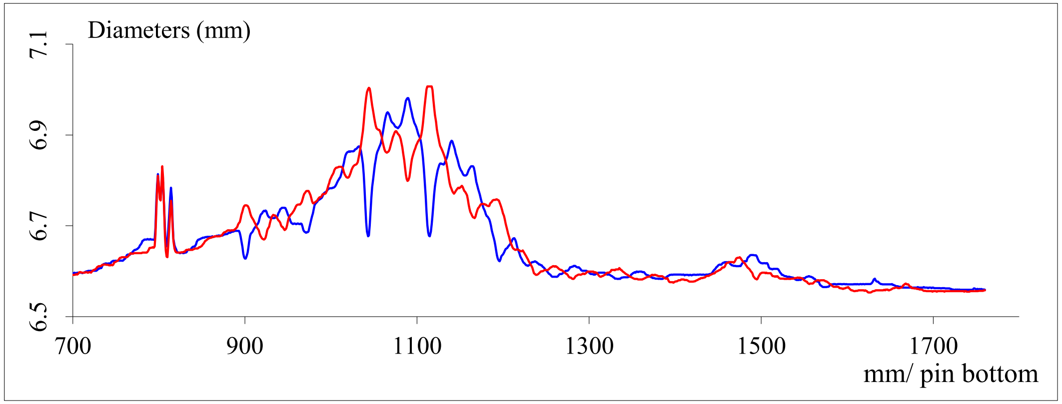

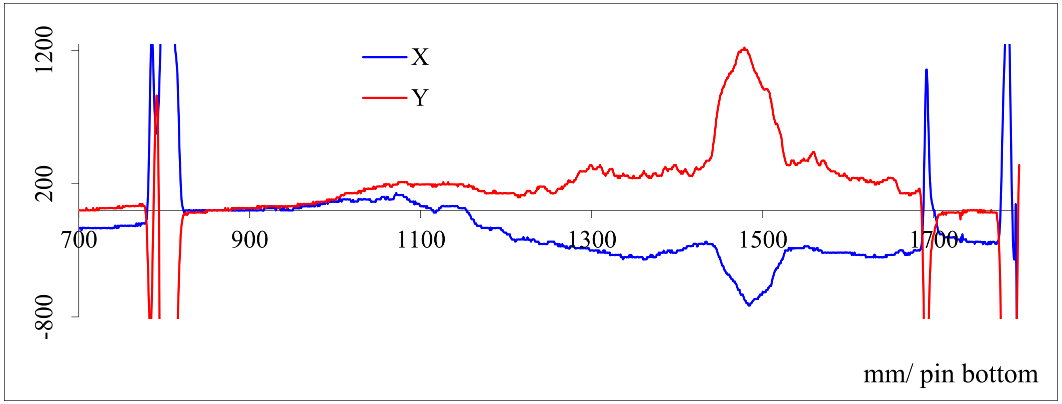

- gammascanning → axial distribution of gamma emmitting isotopes
- diameter measurements → steel swelling + ovalizations + possible impact of inner corrosion or local accumulations
  the high strain areas are not at PPN, effect of neutron flux + temperature
- Eddy currents, cladding defects, mainly inner corrosion

Non Destructive Examinations: Gammascanning,

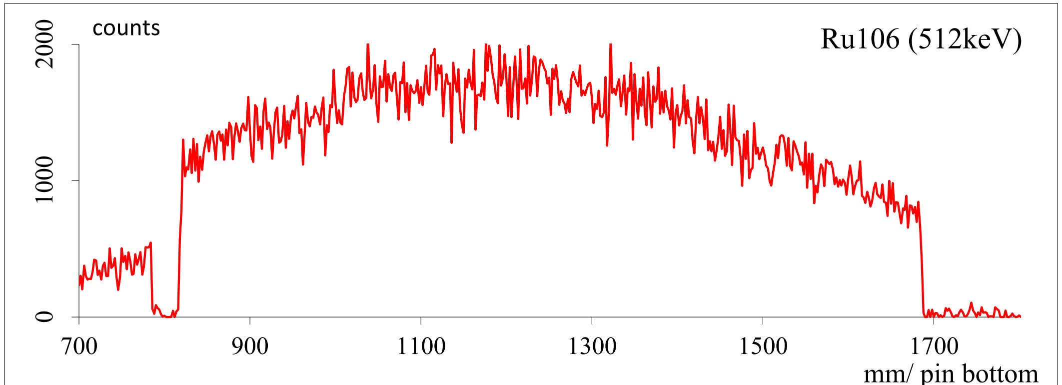

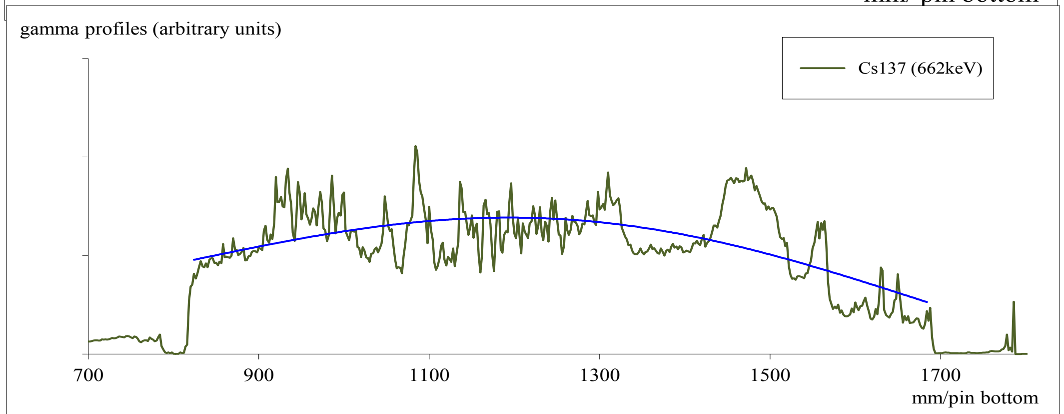

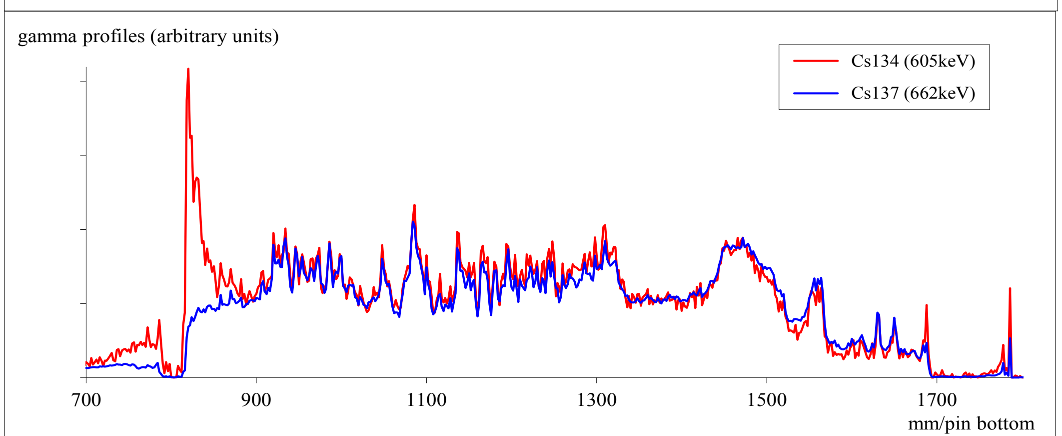

- gammascanning → axial distribution of gamma emitting isotopes
- what can be measured depends on the cooling time :

^{106}Ru period is year

→ after 9 years of cooling since the shut down of Phenix, the Ru activity has been divided by 512, Ru axial profiles are no longer measureable in Phenix pins gammascanning → axial distribution of gamma emitting isotopes

- Gives access to the fuel column lengths
- Cs profiles show axial movements, and both similarities and differences between the two gamma emitting Cs isotopes

(^{137}Xe 3.82 min, ^{133}Xe 5.25 days) → partly Cs, partly Xe movements

Non Destructive Examinations: Gammascanning,

- gammascanning → can say a lot, with high differences from one irradiation to the other

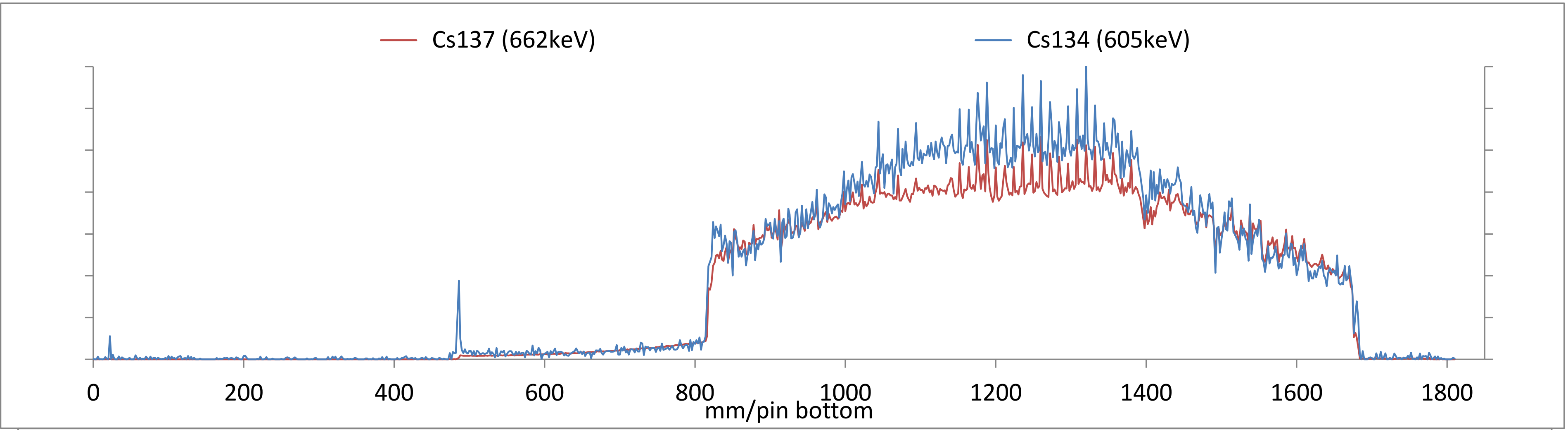

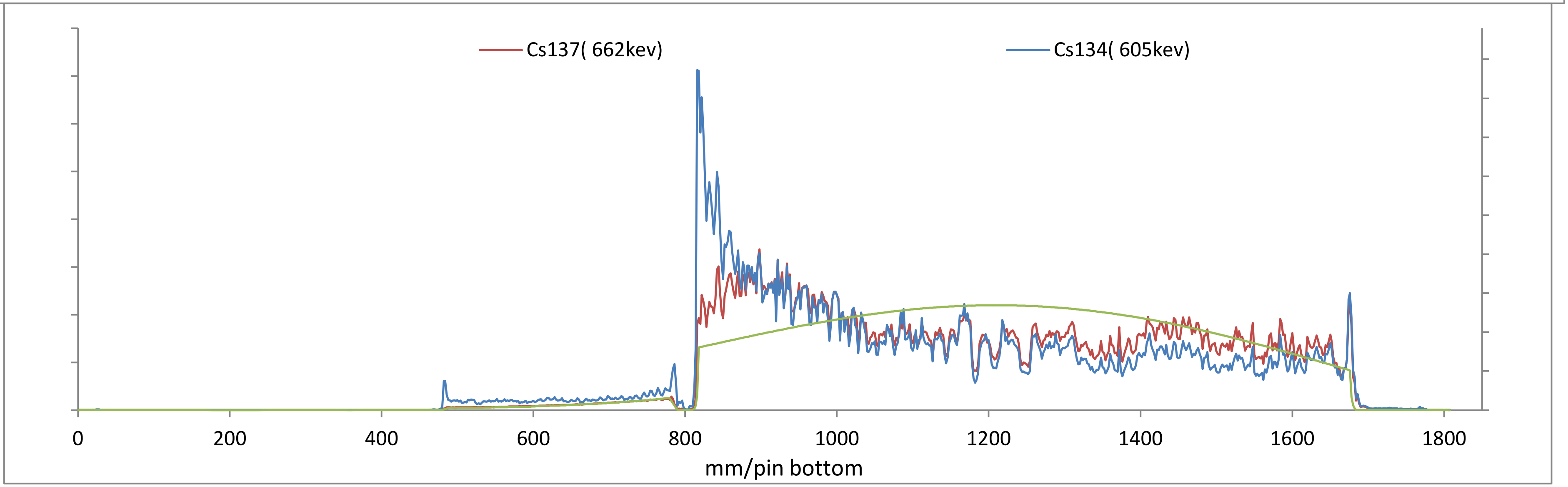

Early in life corrosion

- Cases of early in life clad failures are good to keep in mind:
  - failures after one or two weeks of irradiation
  - in pins with a high linear rate (≥450 W/cm^{-1})

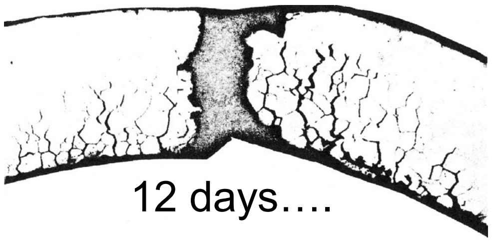

12 days….

- **PIE**
  - Gammascanning → volatile fission product accumulation at both ends of the central hole (where ruptures occur)

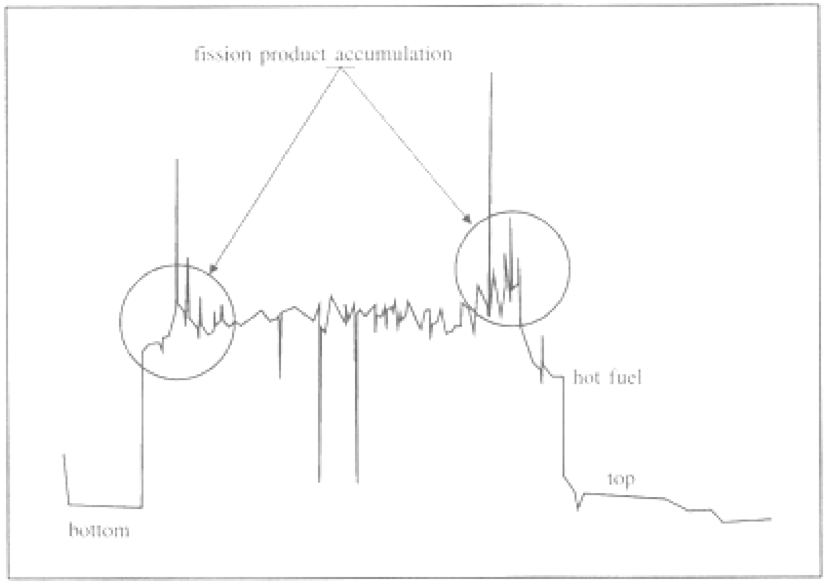

- Optical microscopy → very high intergranular corrosion on the inner cladding surface

- **Lab experiments**
  - intergranular attack of stainless steel occur when Cs/Te < 2

- **Neutronics**
  - Cs yield > 5 times Te yield !!!
  - but because of the complex decay chains, at BOL, while the future Cs is still I or Xe, Cs/Te ratio can be < 2!

- **Solution**

Lower LHR at BOL → lower volatile fission product migration when Cs/Te is low
A sort of vaccination

Pin puncturing

- → measuring the amount of gas in the free volumes of the pins
- → measuring the elemental and isotopic composition of the gas
- → measuring the free volume in the pin

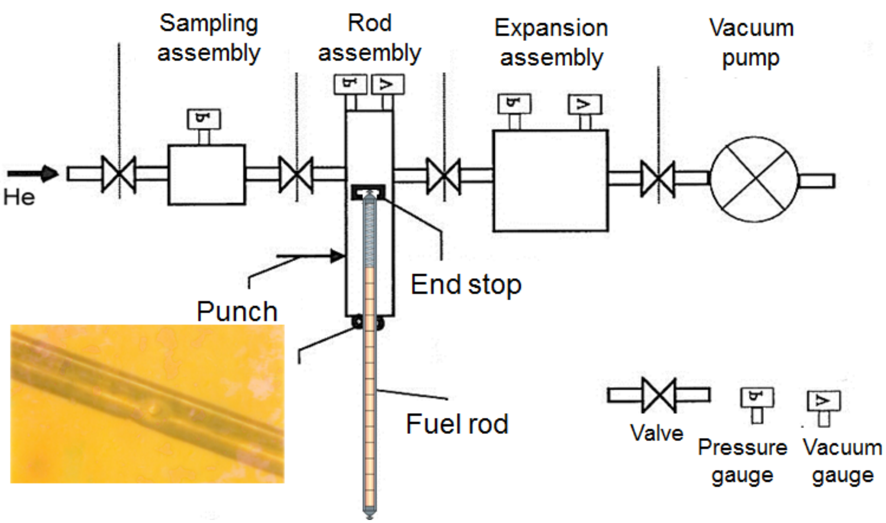

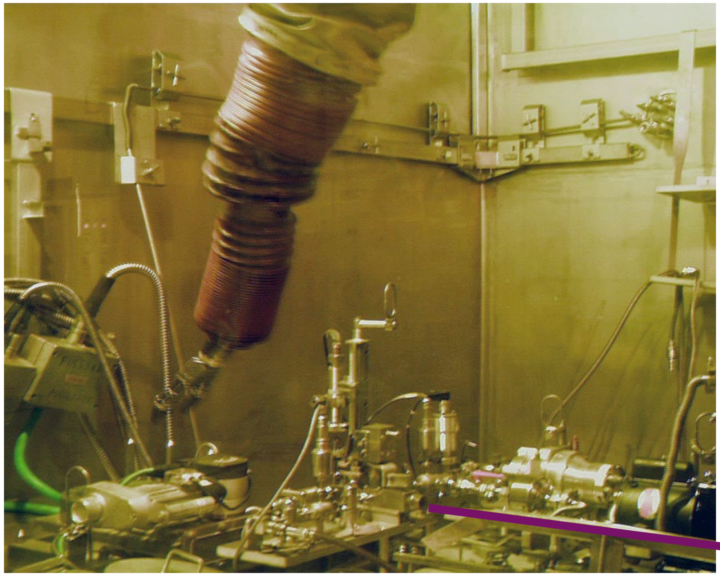

Pin puncturing

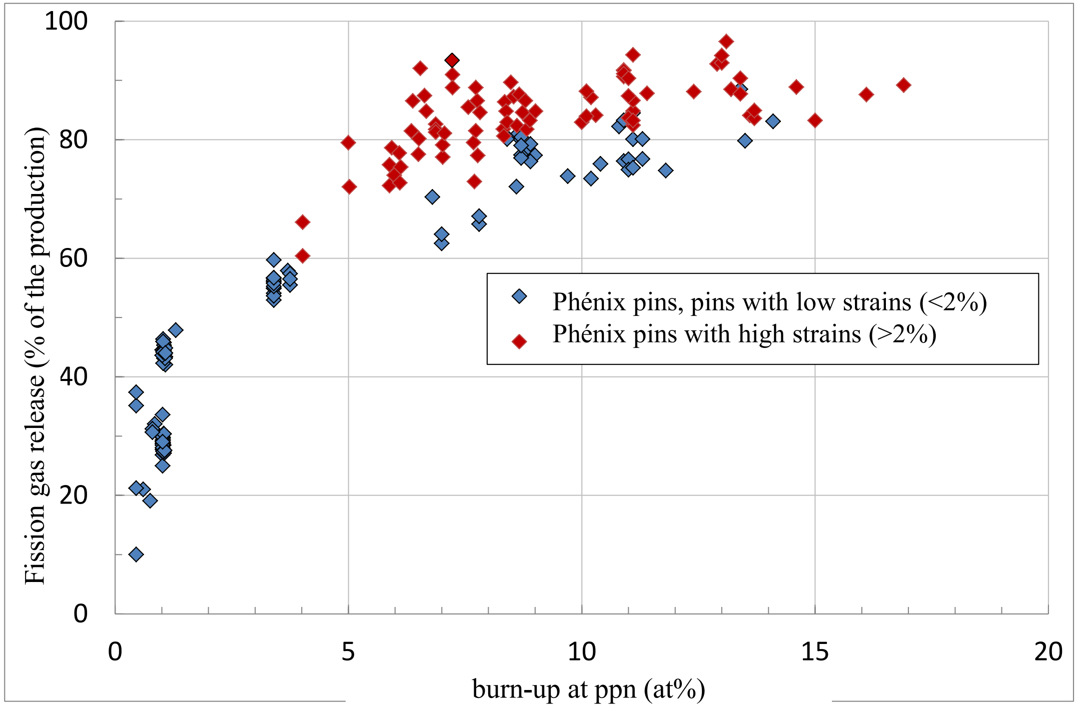

- High fission gas release even at low burn-up → the free volumes must be adapted to a total release of the fission gases at the target BU
- Slightly higher release in pins with a high strain. Why?

For comparison, typical PWR FGR%

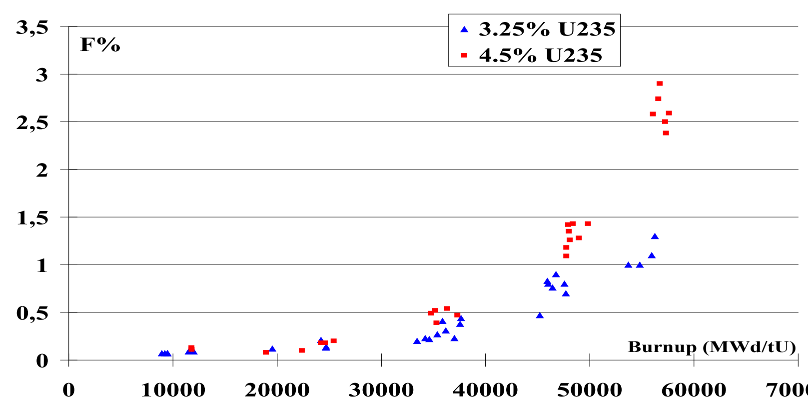

Pin puncturing

- Conductivity of gaseous mixture depends on its composition

He "good" conductivity

Xe and Kr low conductivity

$$\lambda_{gas} = \sum_{j=1}^{n} \left[\frac{\lambda_j}{1 + \sum_{k=1}^{n} w_{jk} \frac{c_k}{c_j}} \right]$$

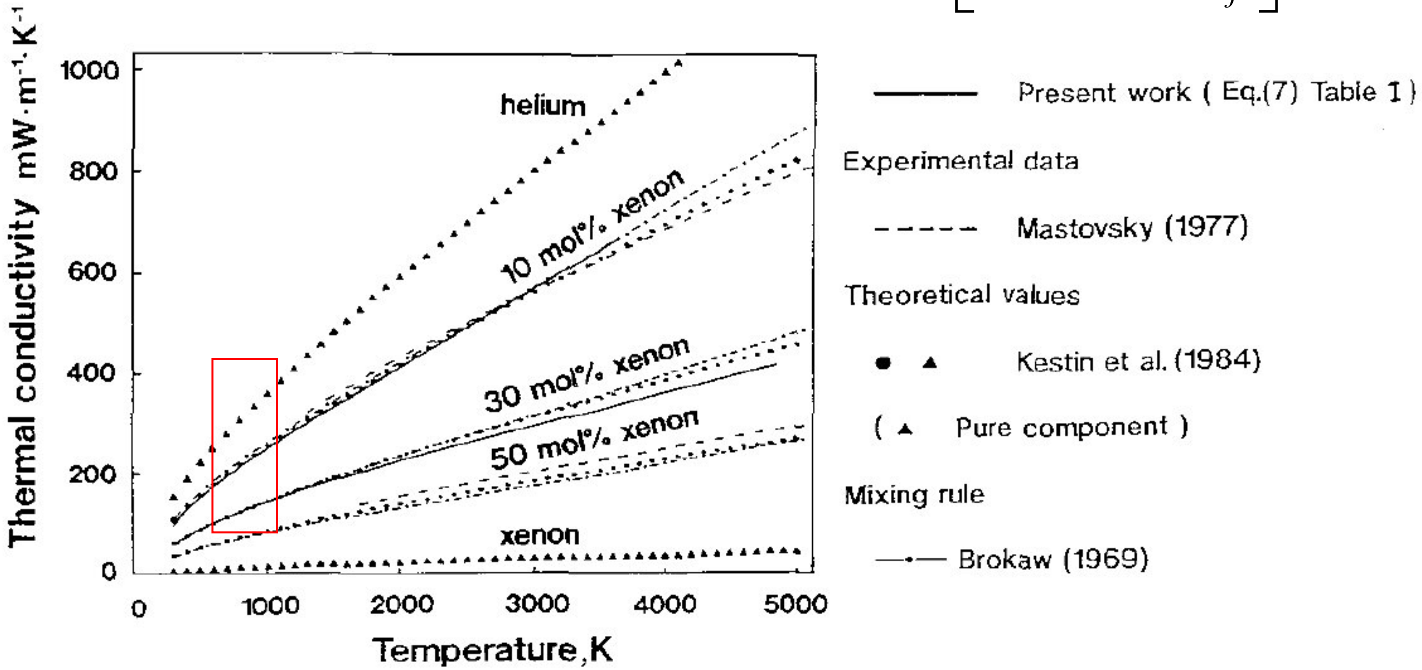

Fig. 6. Thermal conductivity of helium–xenon mixtures as a function of temperature.

Optical microscopy

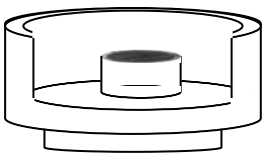

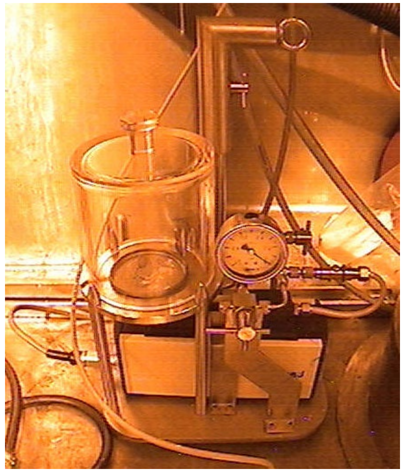

Embedding,
grinding
and polishing

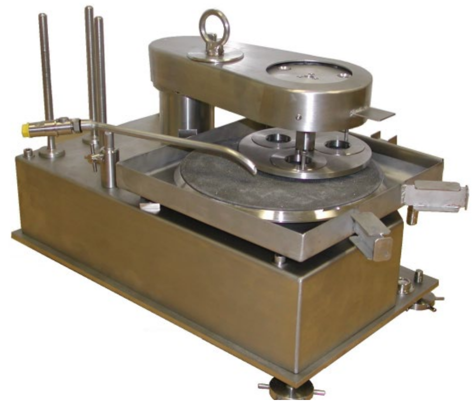

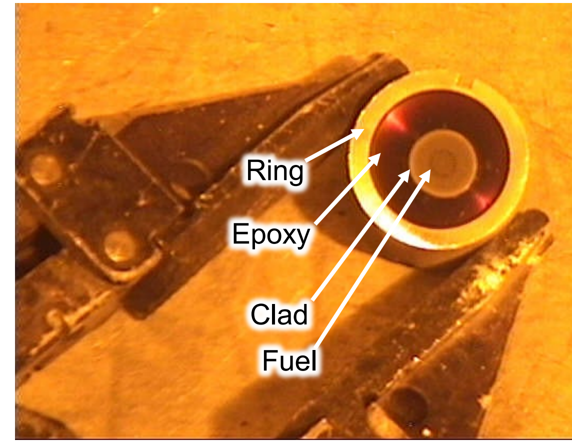

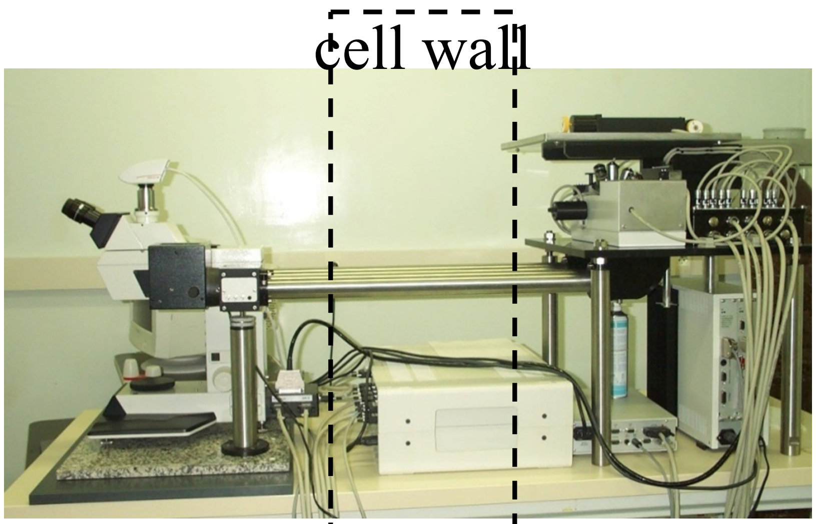

Optical Microscopes

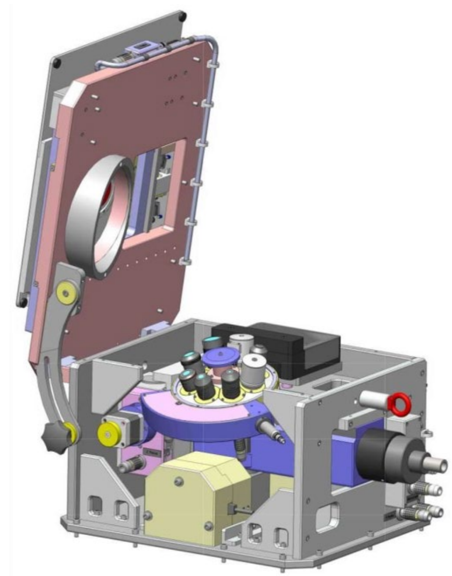

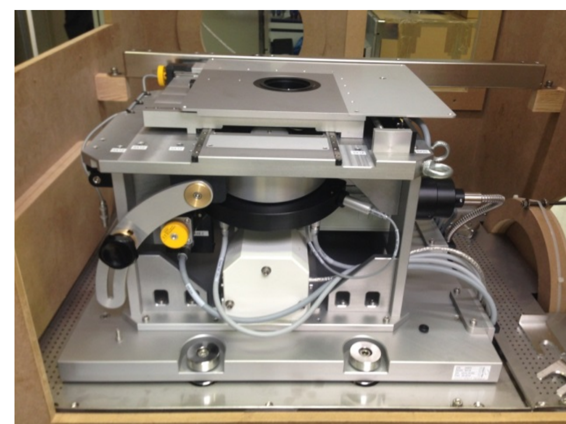

Optical microscopy

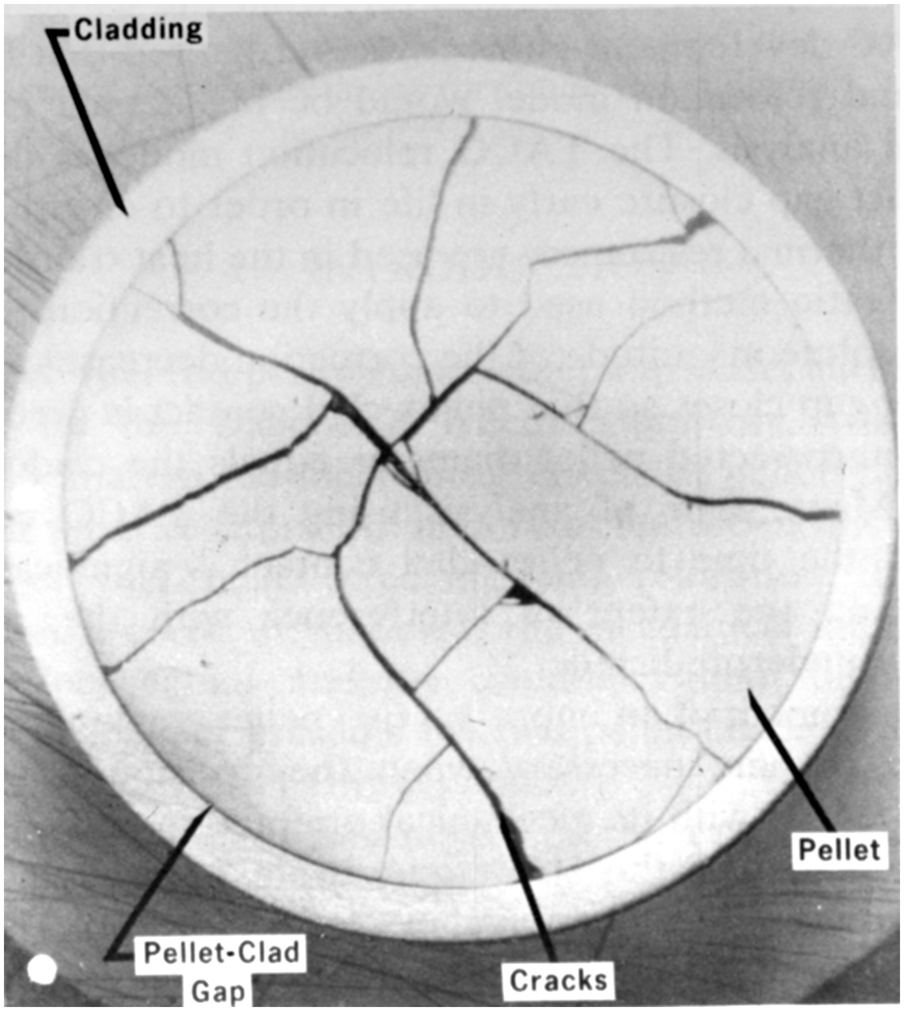

Walton (1983)

Higher thermal expansion in the center
→ tension stress on the periphery
→ radial cracks

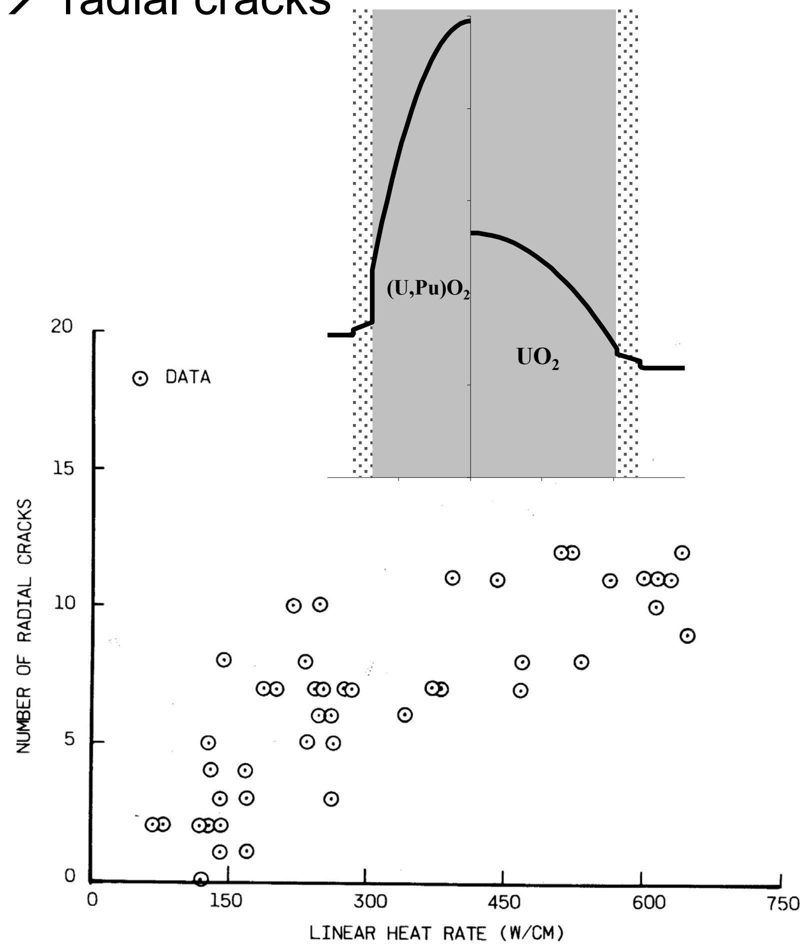

Number of radial cracks as a function of power. Low burnup data BU < 5 GWd/mtU.

Optical microscopy

Cavities (pores and cracks) move up the temperature gradient by evaporation / condensation, lenticular pores
→ central hole, columnar grains

PHENIX - 13 at %

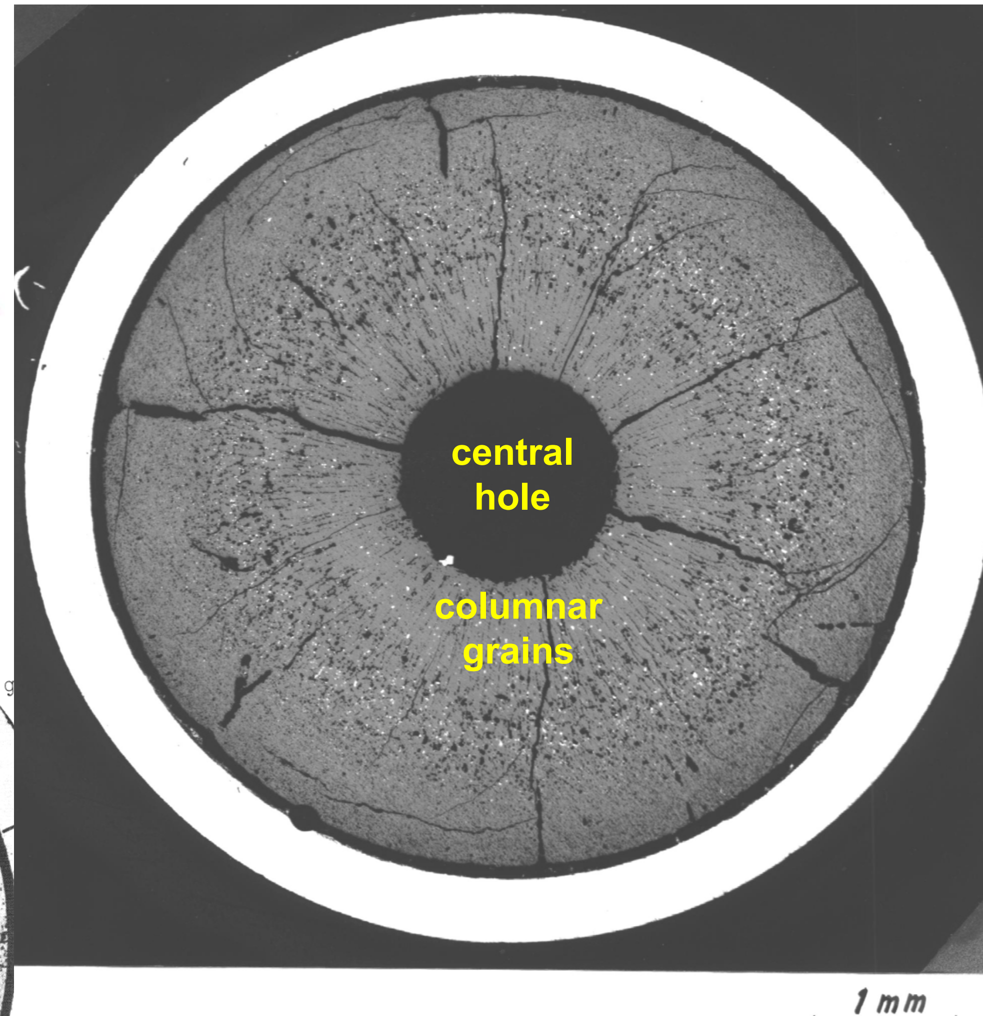

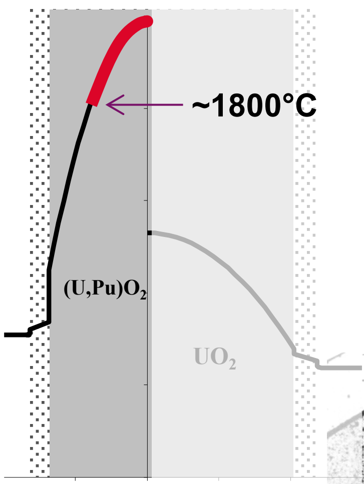

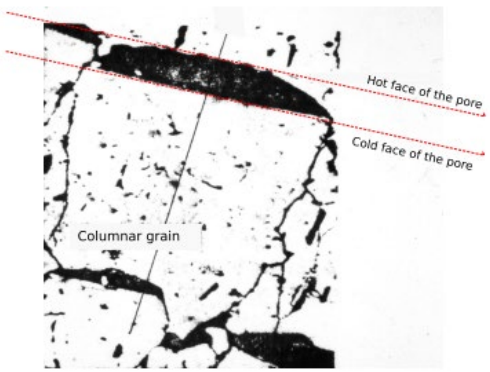

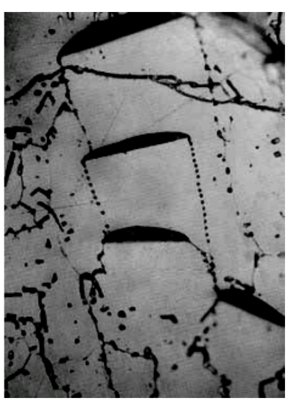

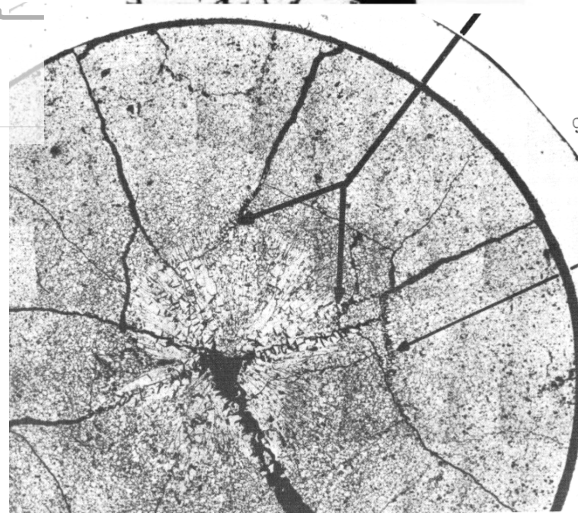

RAPSODIE 4h 380 W/cm

(See M.J. Welland Comprehensive nuclear materials 2012)

Optical microscopy

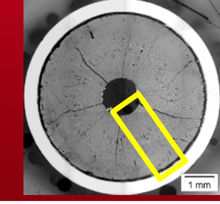

before chemical etching

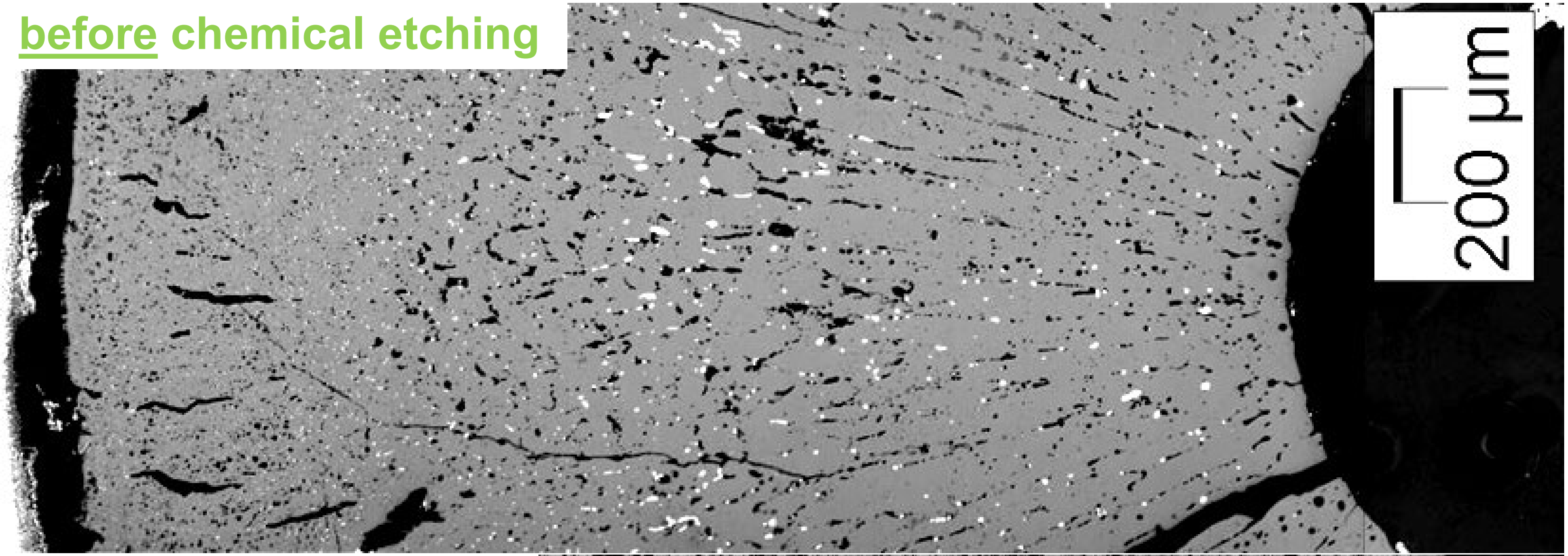

After chemical etching

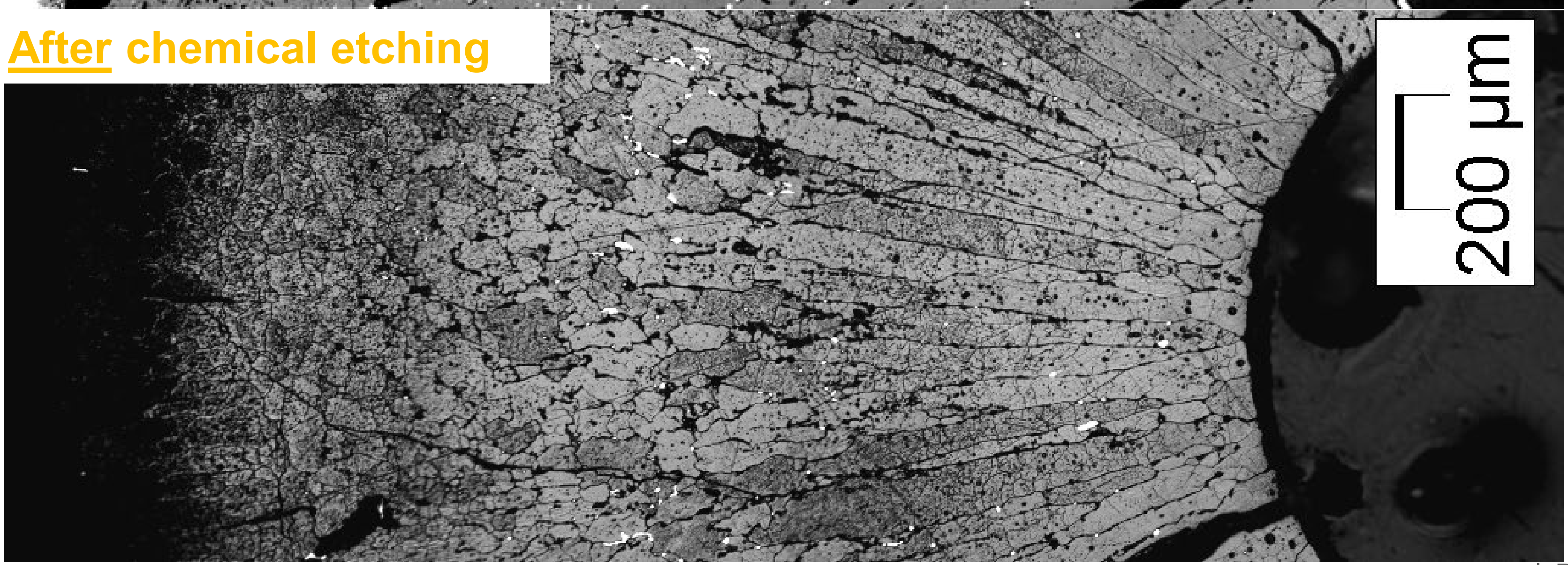

DE LA RECHERCHE À L'INDUSTRIE

Optical microscopy

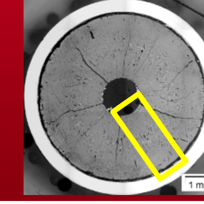

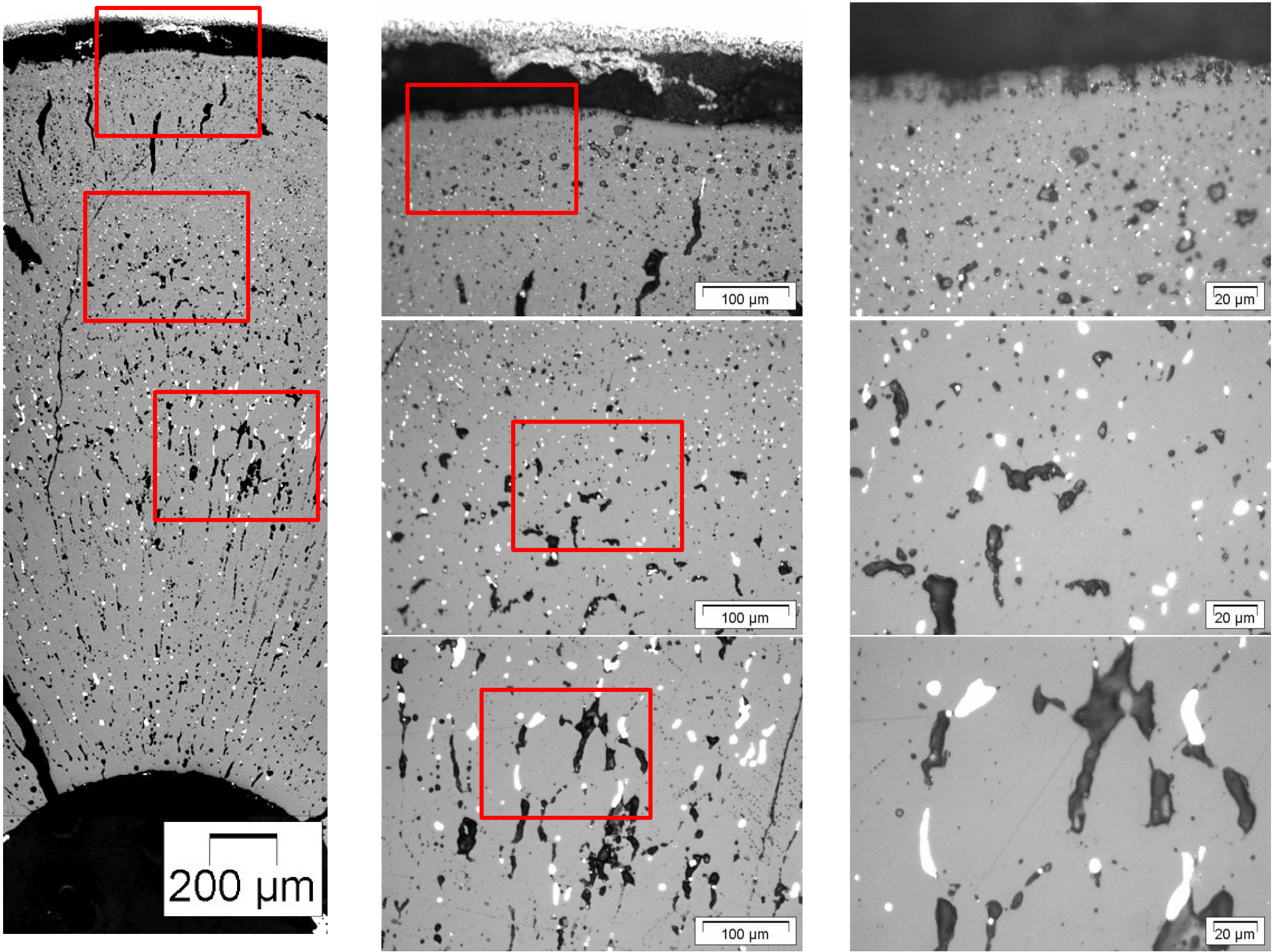

1R

0.8R

0.55R

Optical microscopy

Batelle 1966 (USA)

Optical microscopy

- differences along the same fissile column

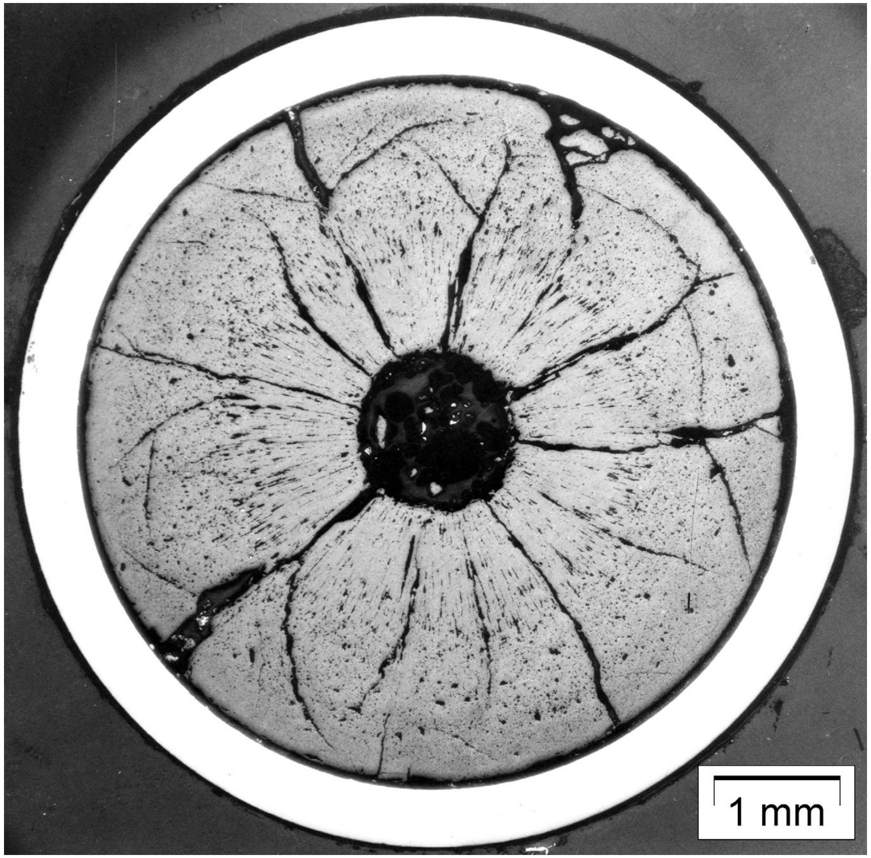

310 mm/fuel column bottom

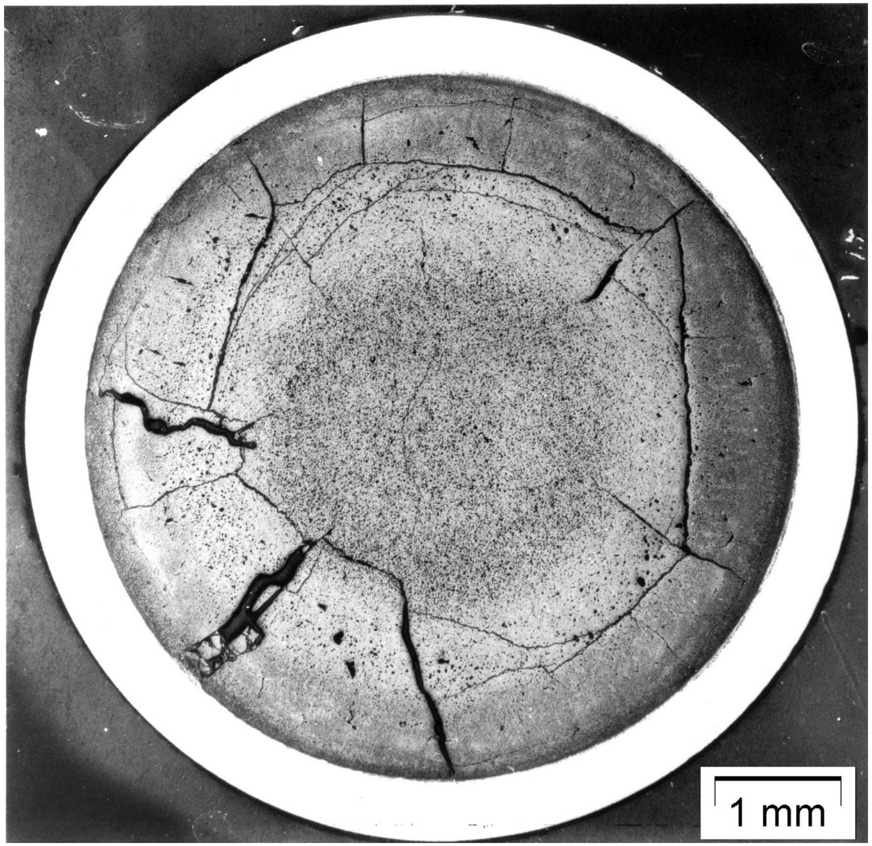

678 mm/fuel column bottom

Optical microscopy

- Internal corrosion (ROG)

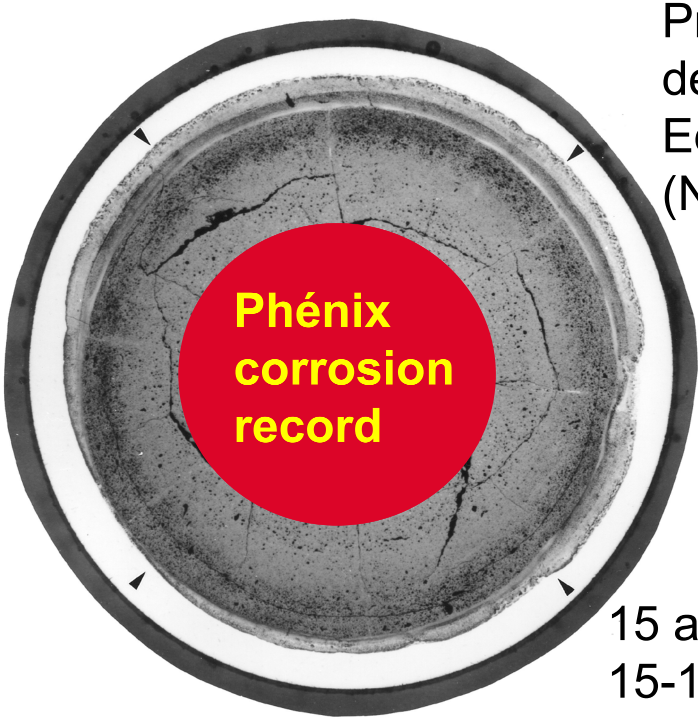

Phénix corrosion record

Previously detected by Eddy currents (NDE)

15 at%
15-15 Ti

- Corrosion at fissile-fertile interface (RIFF)

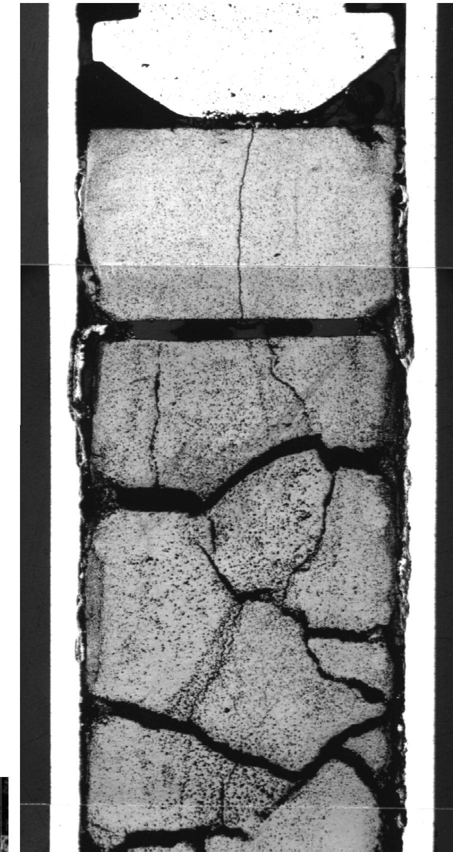

Zones with an accumulation of volatile fission products

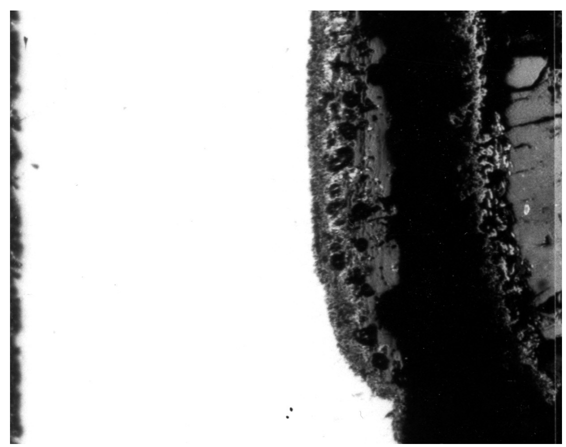

Optical microscopy

- HBS high burn-up structure formation on the pellet periphery

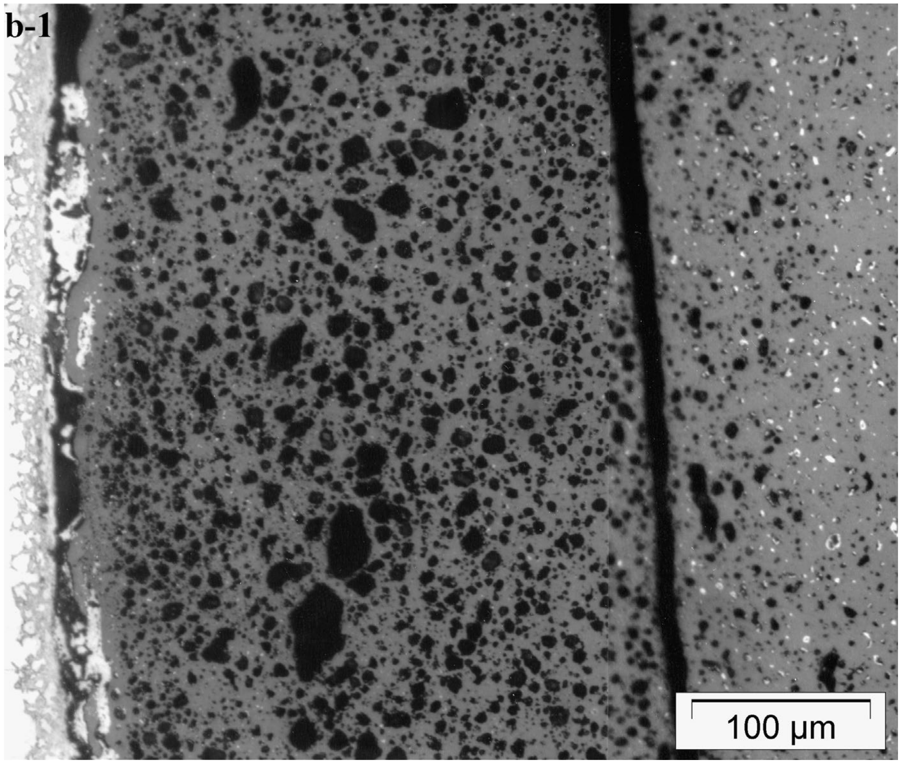

no chemical etching

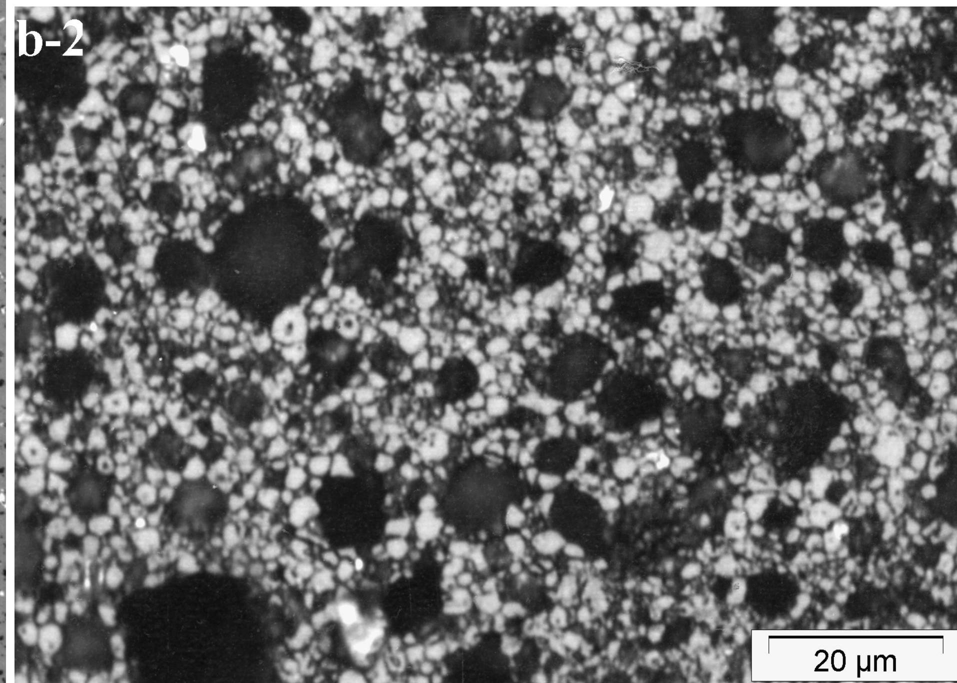

after chemical etching revealing the grain boundaries

- Similar to the HBS in LWR fuels (rim effect), larger sub-grains linked with the higher irradiation temperatures (similar to the larger sub-grains found in MOX-MIMAS Pu agglomerates away from the periphery

Optical microscopy + α-radiography

α-radiograph on a BN600 Vipac fuel
Homogeneization of the Pu in the center

A. F. Gratchyov et al
JNST 2007

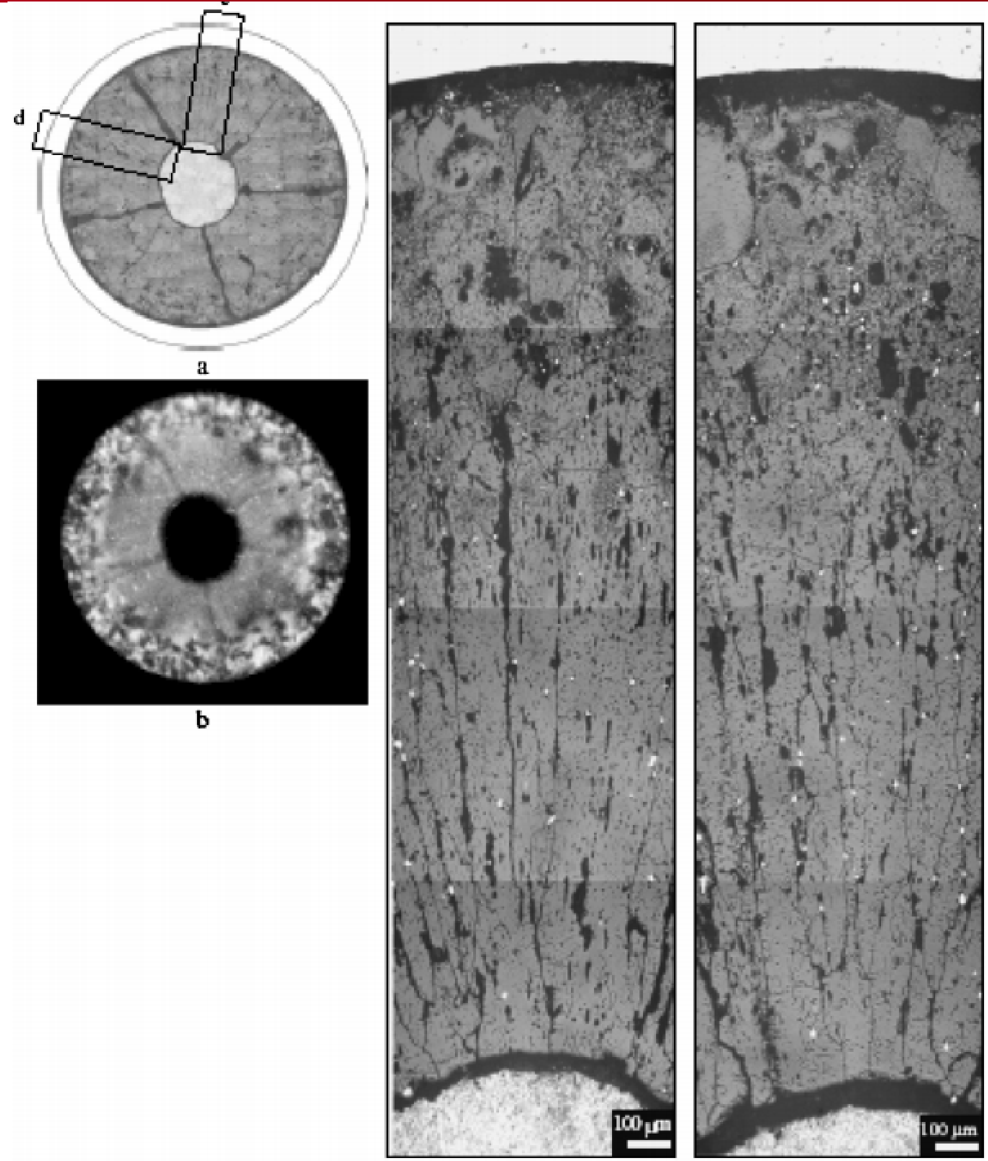

c d

Optical microscopy + α-radiography

W. J. Lackey et al.
Nuc. Tech. 1972

Higher Pu content around the central hole, Pu homogeneization in the columnar grains, lower Pu content deposit around the spheres in intermediate zone

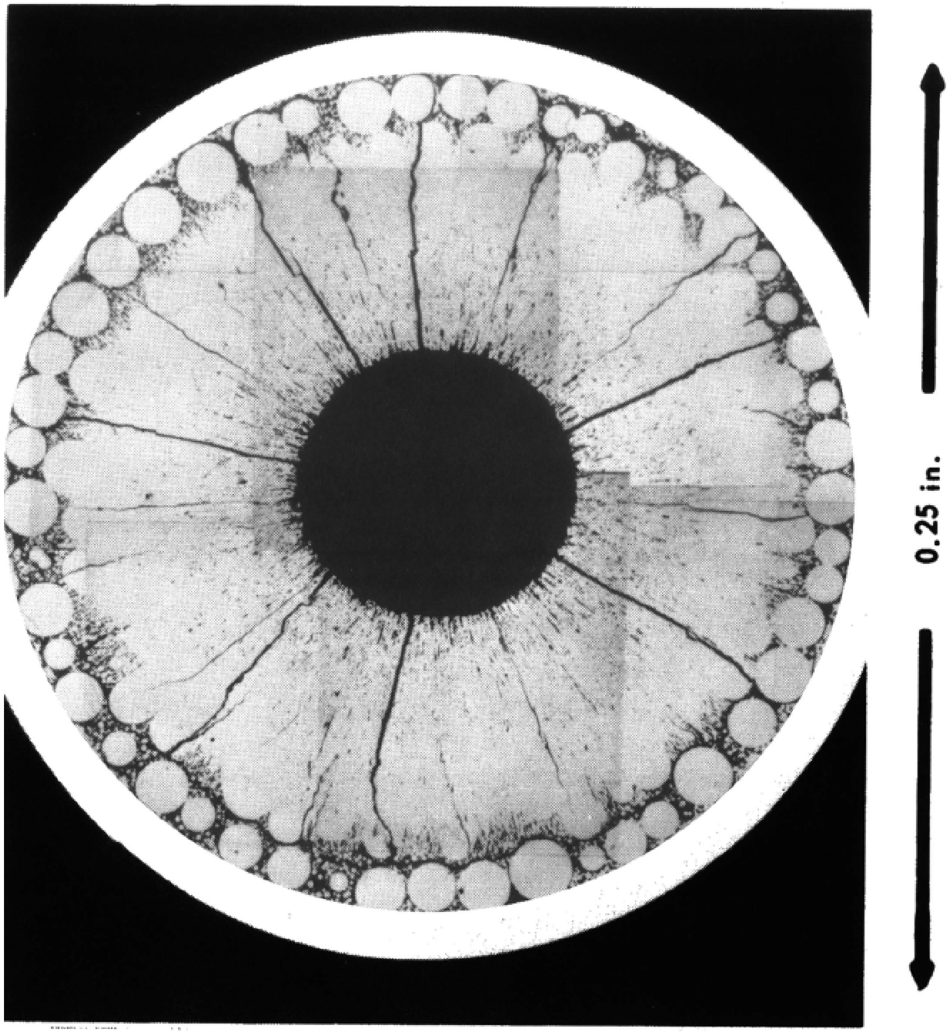

PHOTOMACROGRAPH

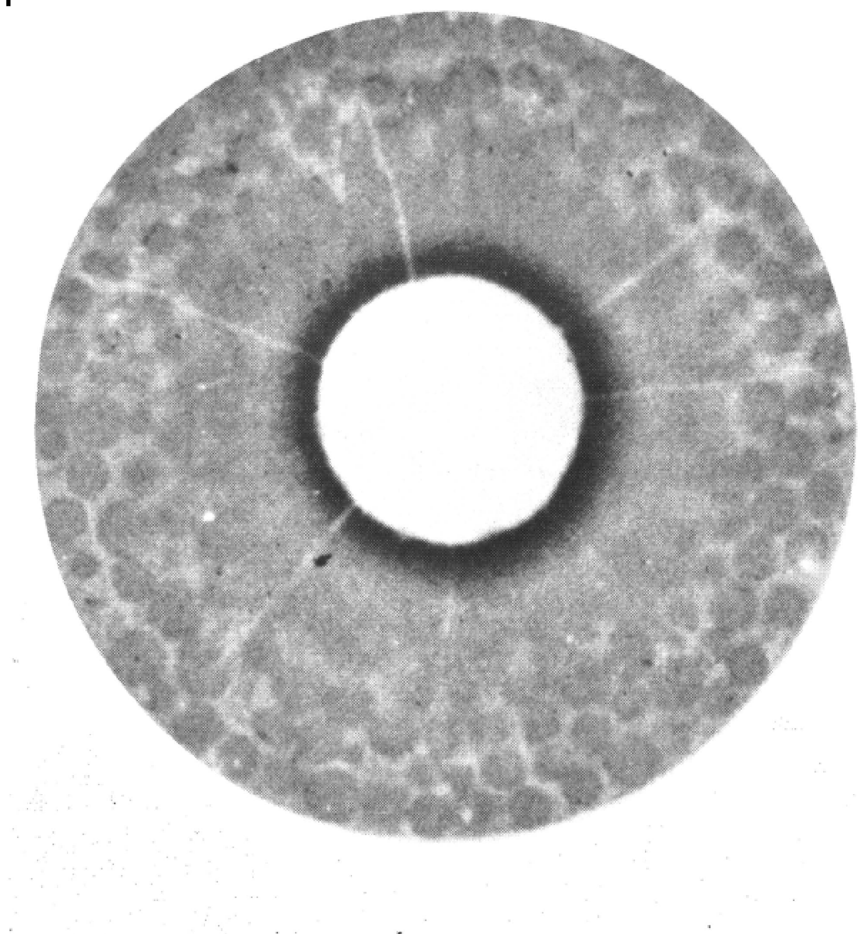

α AUTORADIOGRAPH

Scanning Electron Microscope

- images from low magnifications to high magnifications

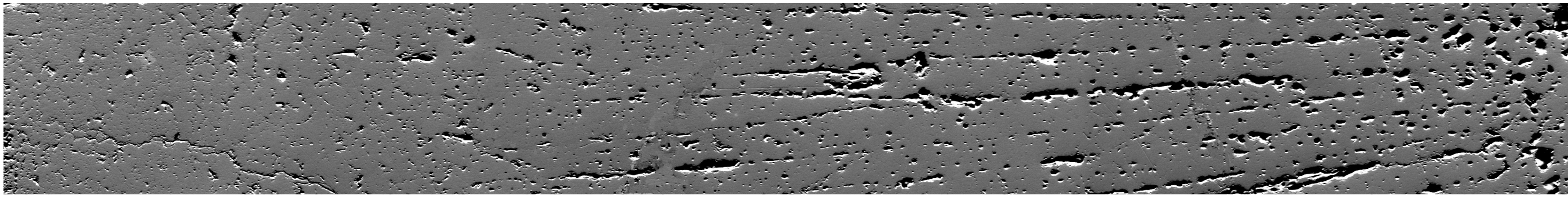

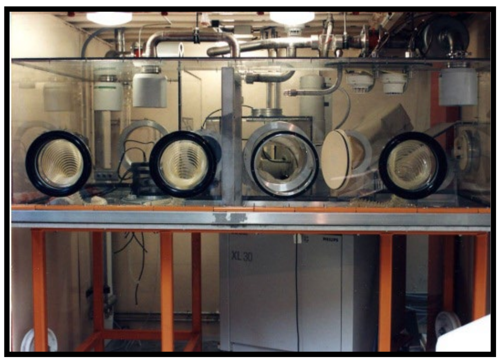

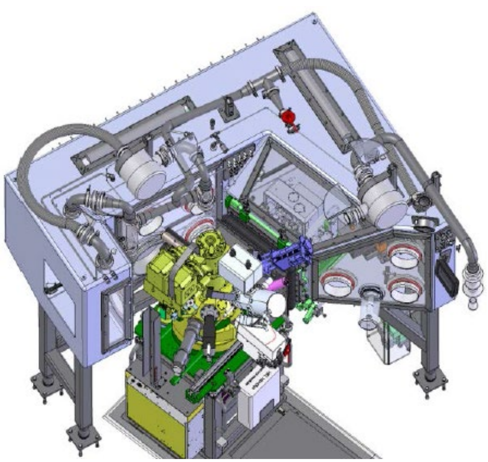

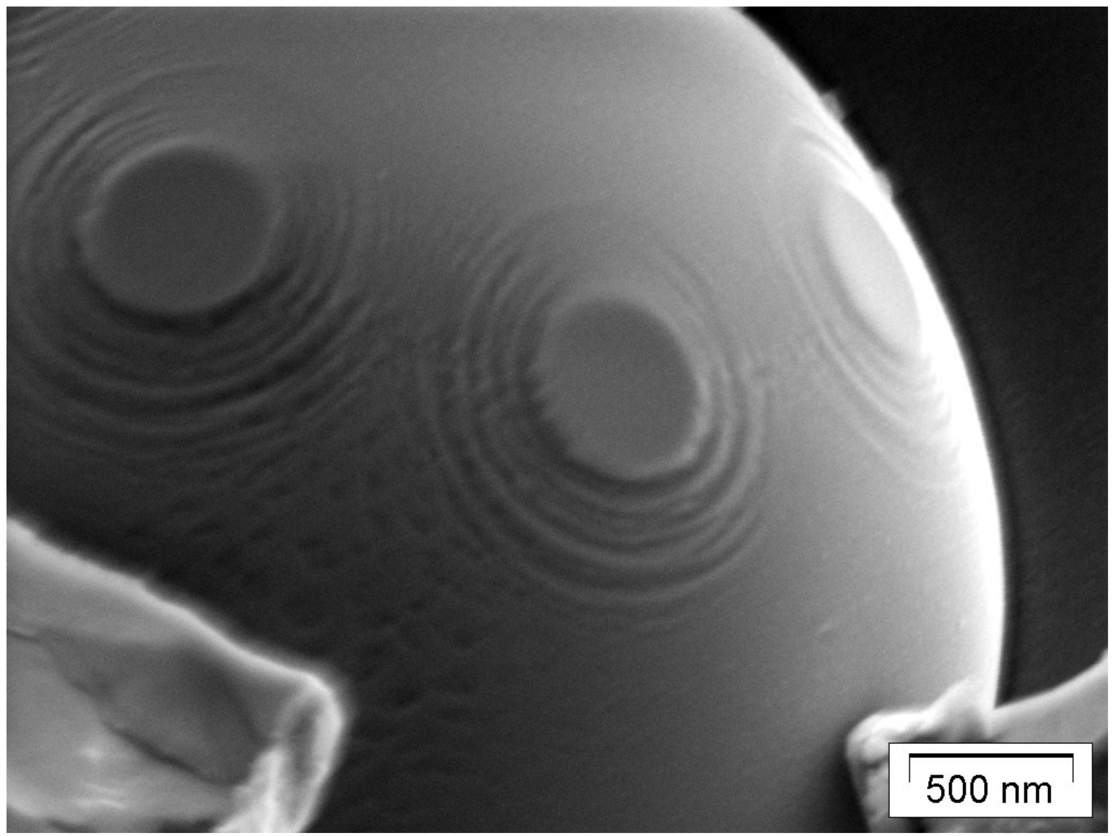

Electron Probe Micro Analyzer

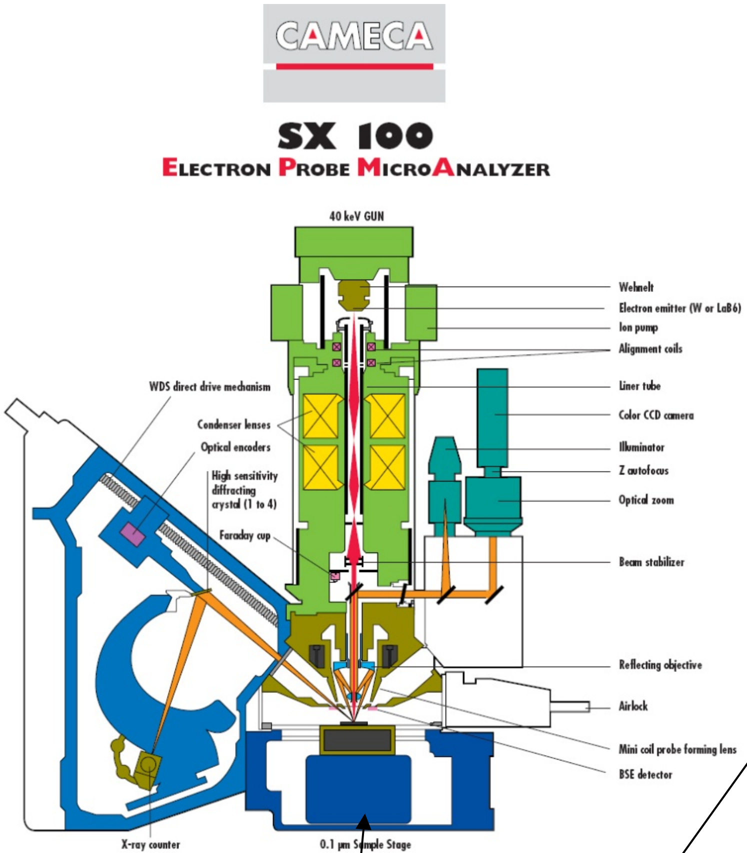

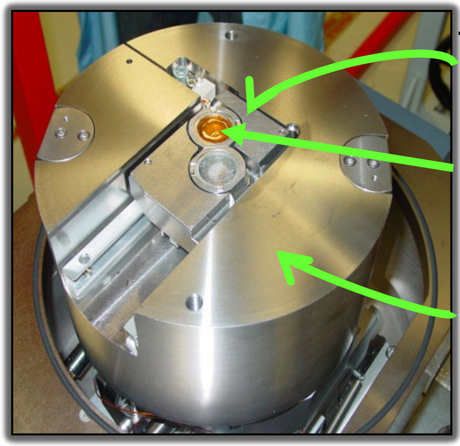

Tungsten shielding

Sample

Tungsten shielding (80 kg)

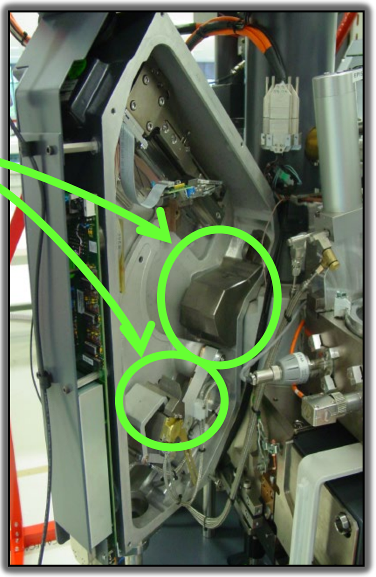

extra shielding between sample and detection

glove box

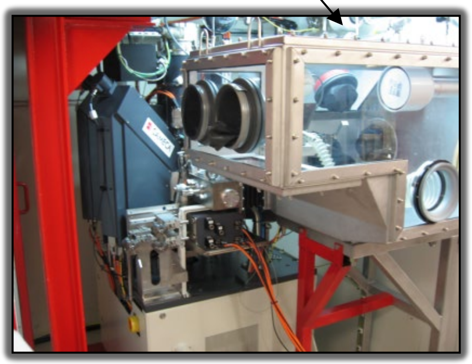

cell wall

Electron Probe Micro Analyzer

- Higher Pu concentrations around the central hole
- Lower Pu concentrations at ~mid-radius
- → The radial power profile (hence the BU profile and the FP concentration profile) is not flat
- → Influence on the temperature radial profile and on the fusion temperature

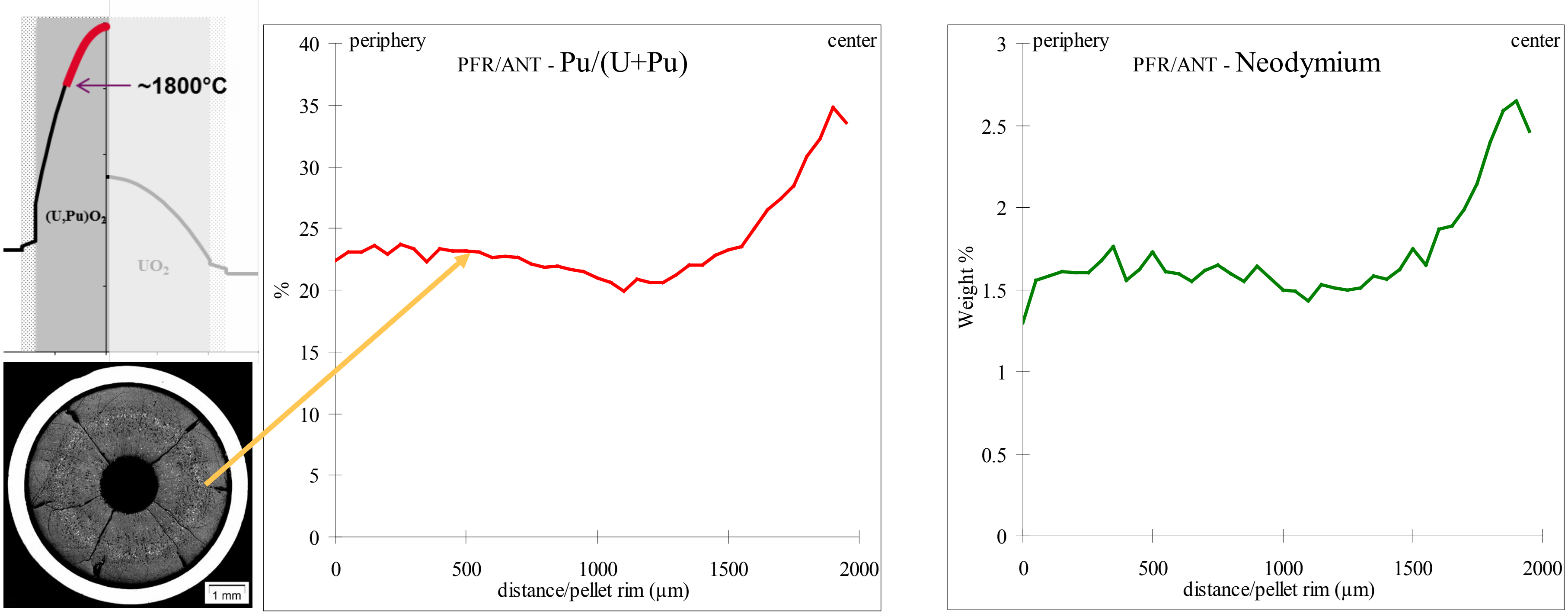

Pu/(U+Pu) radial profile example, EPMA measurement on a fuel irradiated in PFR, Dounreay (UK)

Nd fission product radial profile, consequence of the Pu redistribution at the beginning of the irradiation

Temperatures again

- However, the restructuring and central hole formation → decrease of the central temperatures, mainly due to the gap decrease

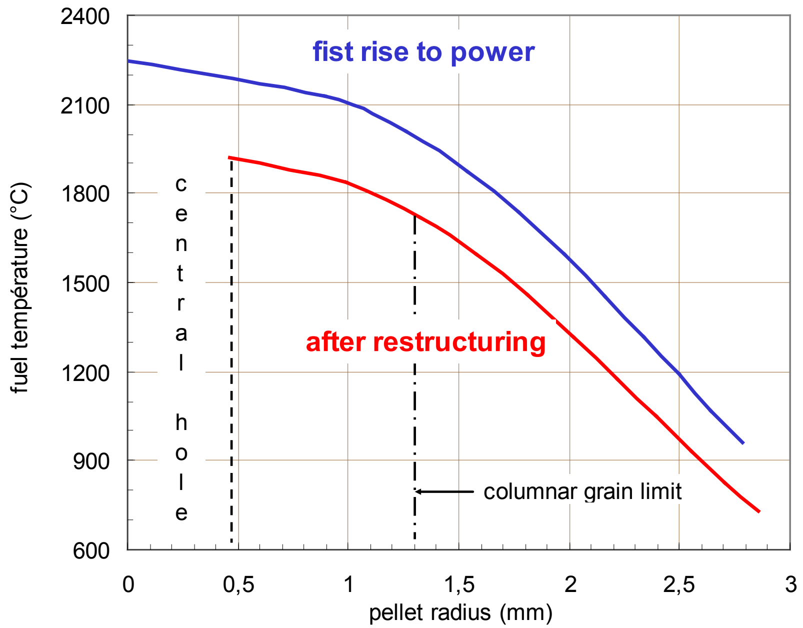

Electron Probe Micro Analyzer

JAEA experiment Am1
(U,Pu,Am,Np)$O_{1.98}$ with 29%Pu, 2%Am, 2%Np
irradiated 24 h in JOYO at 430 W/cm

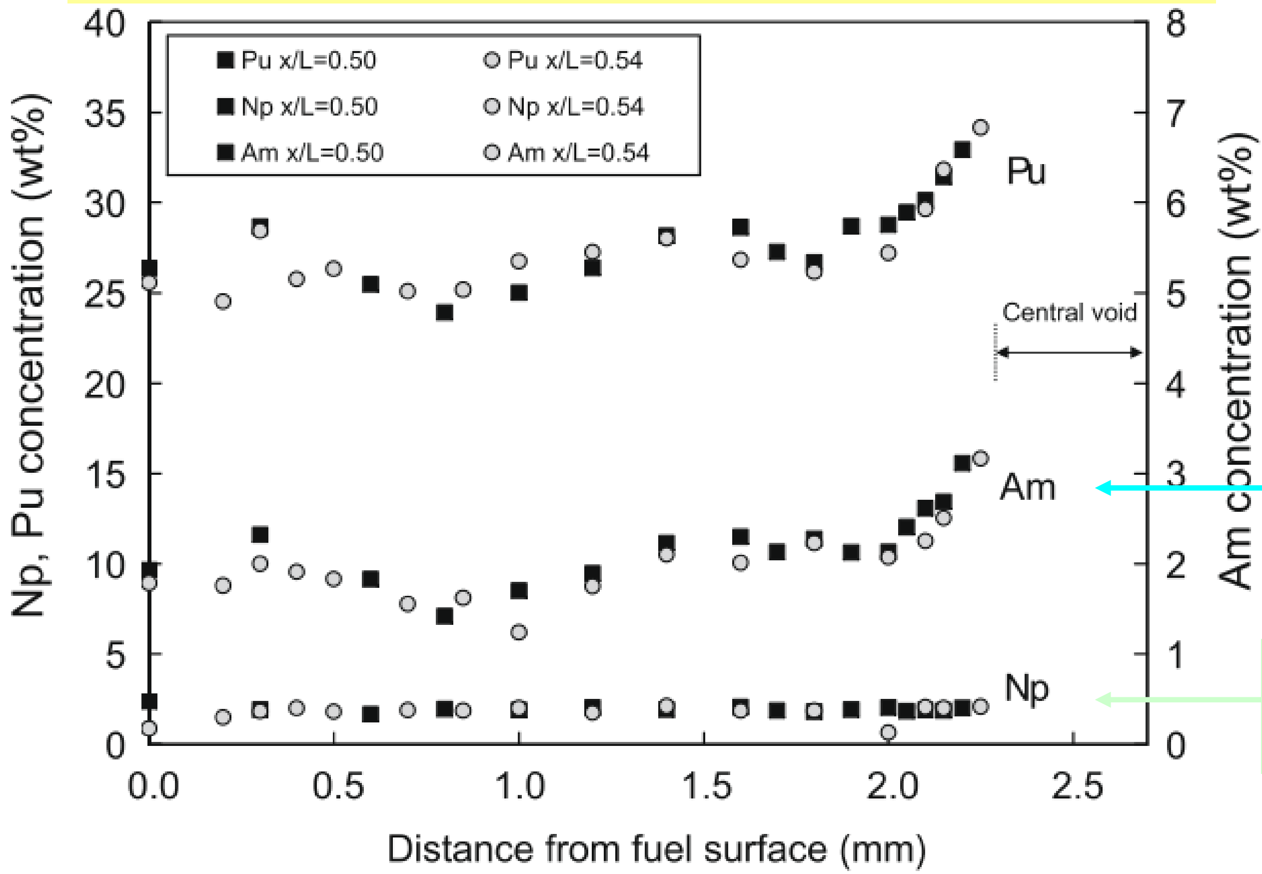

Am enrichment

No redistribution of Np

K. Maeda et al JNM 2009

Electron Probe Micro Analyzer

- Higher Pu concentrations around the central hole
- Lower Pu concentrations at ~mid-radius

Pu map

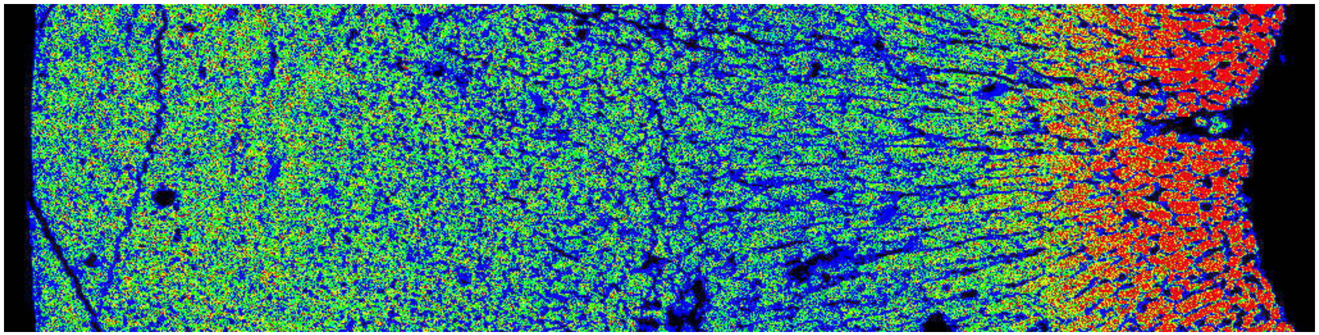

U map

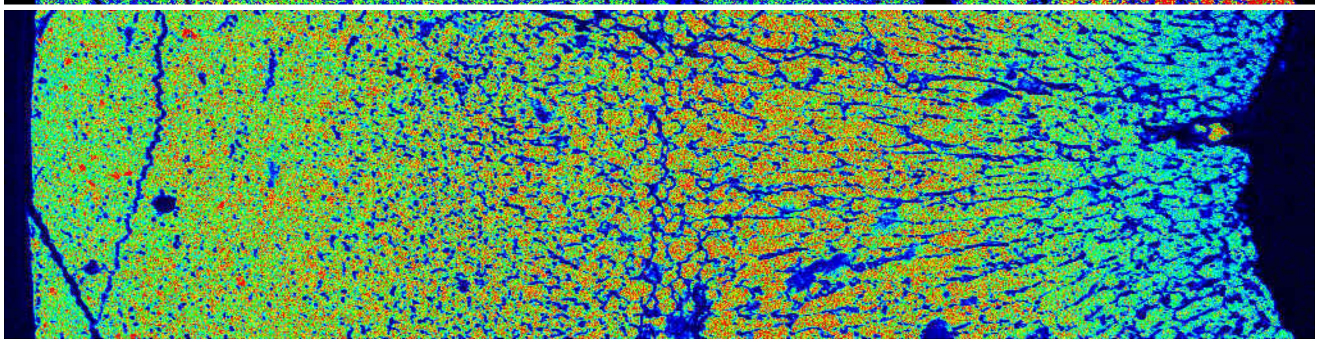

Cs map

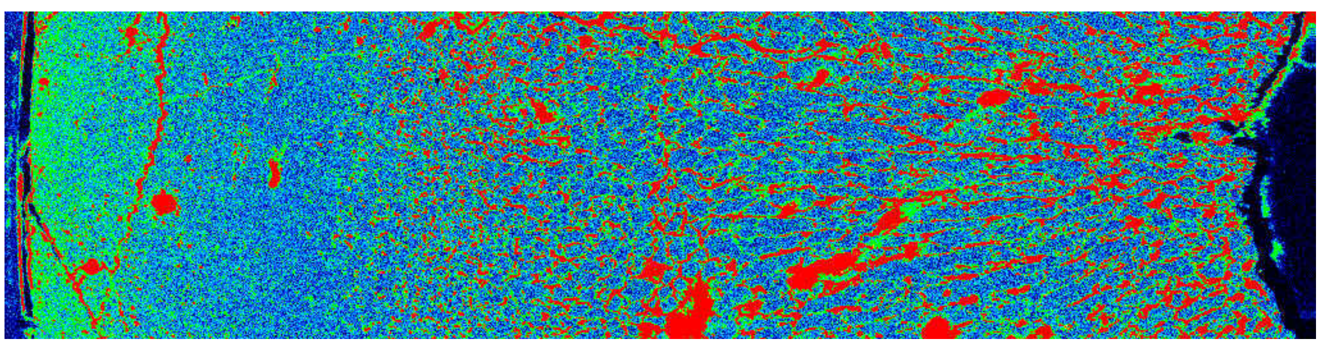

Electron Probe Micro Analyzer

Metallic fission product precipitates

JOG

Mo, Tc, Ru, Rh, Pd…
Pd, Te…

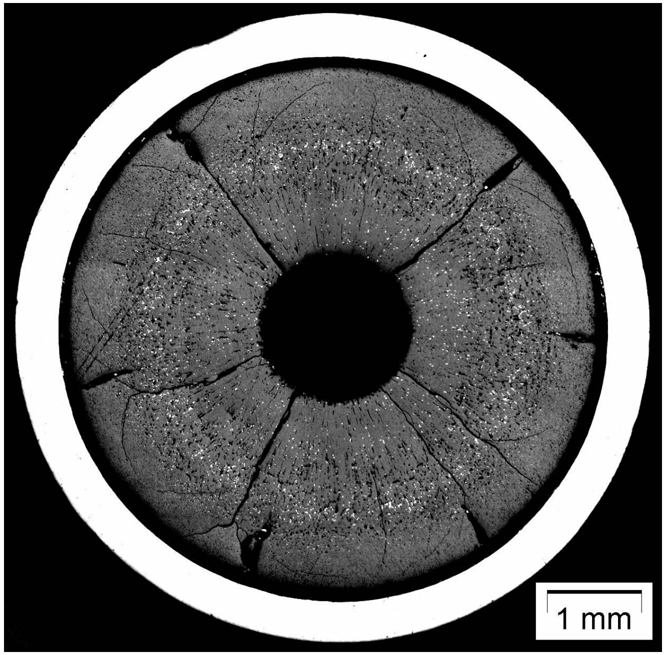

Optical microscopy

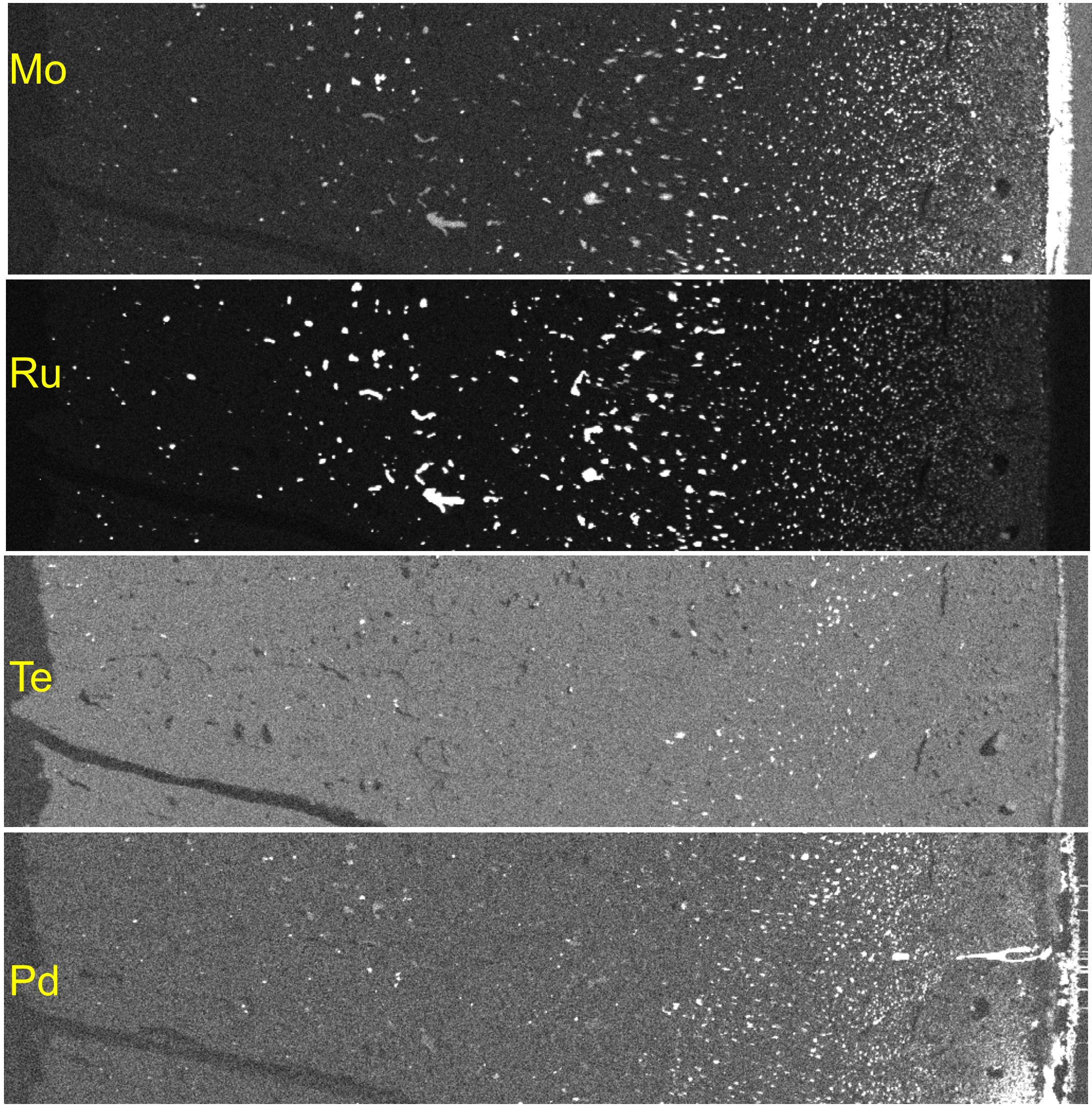

Element maps EPMA

Electron Probe Micro Analyzer

- Oxyde precipitates
  $BaZrO_3$ ....

optical microscopy

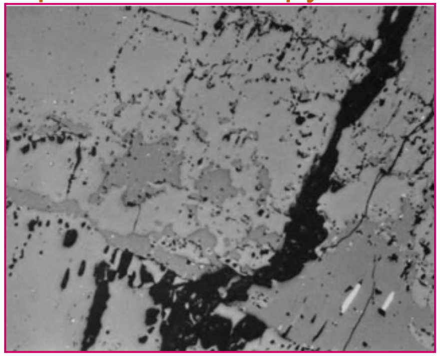

"grey phases"

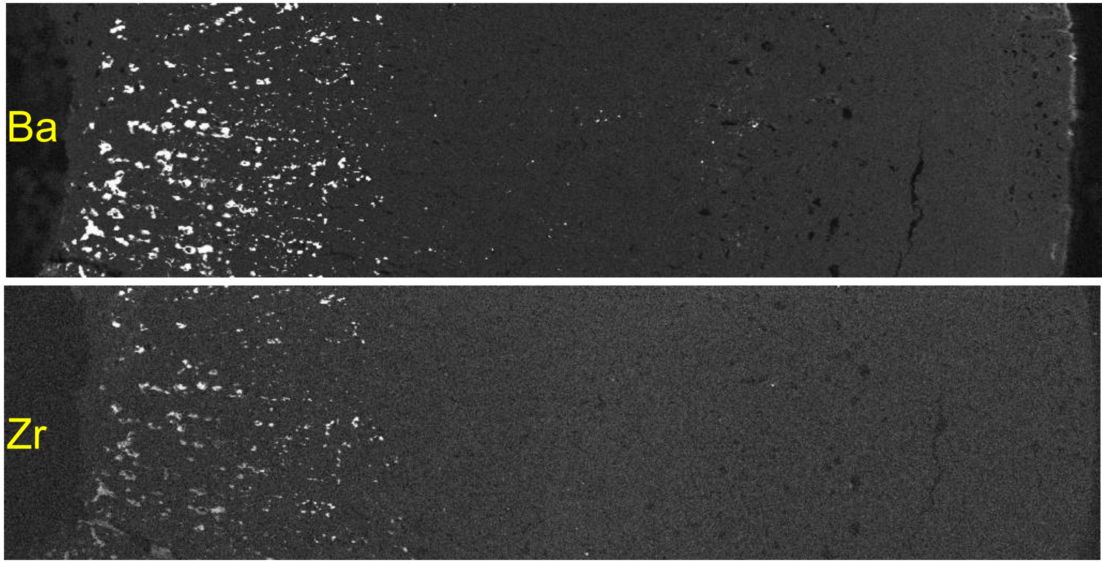

- Changes along irradiation, towards more oxidation (JOG formation)

Mo/Ru ratio in the metallic fission product precipitates in the columnar grain area

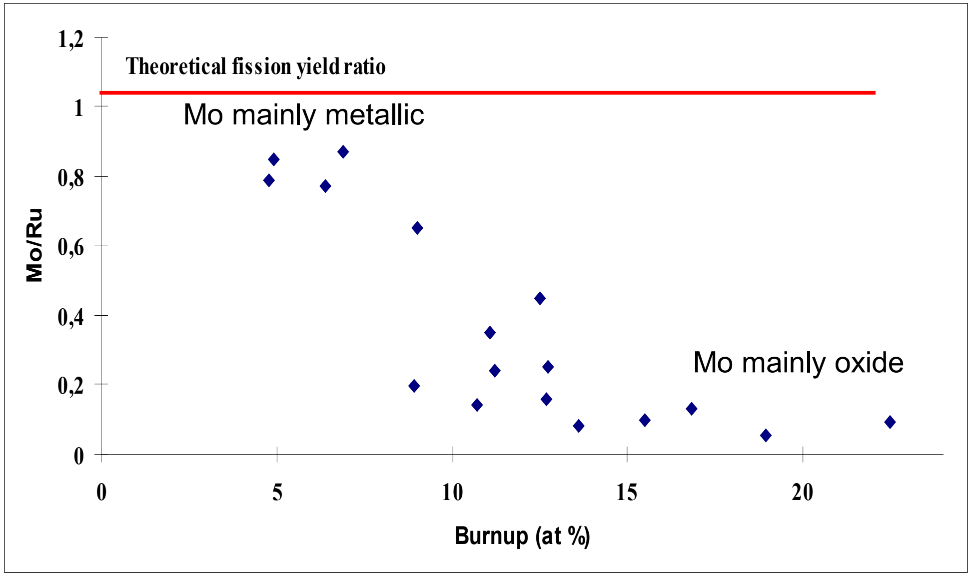

EPMA

Electron Probe Micro Analyzer

- Re-opening of the gap, filling with fission product compounds, sometimes with clad corrosion elements beyond ~7at%

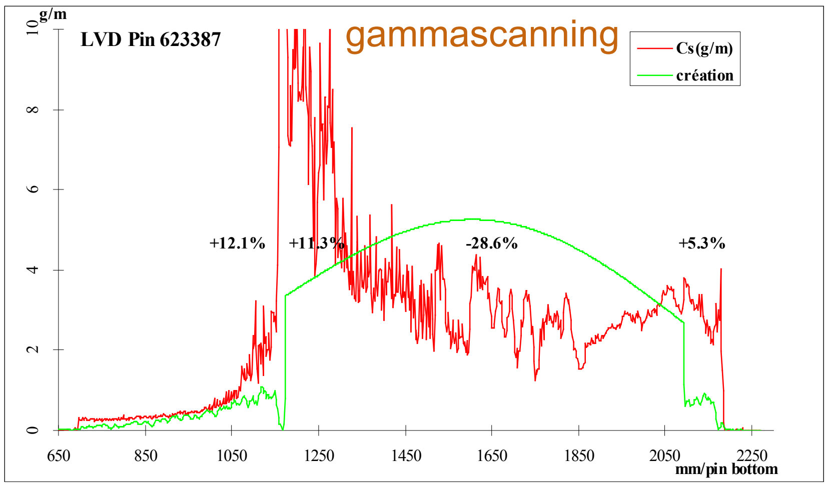

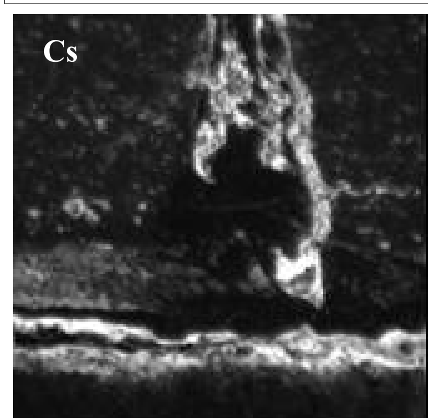

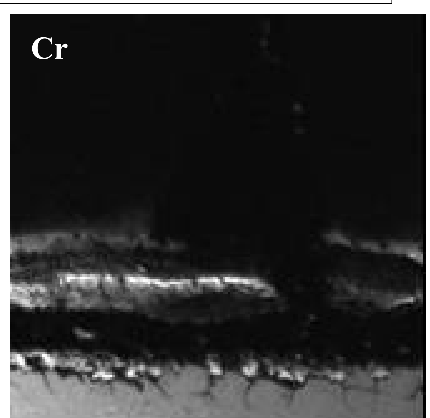

Element maps (EPMA)

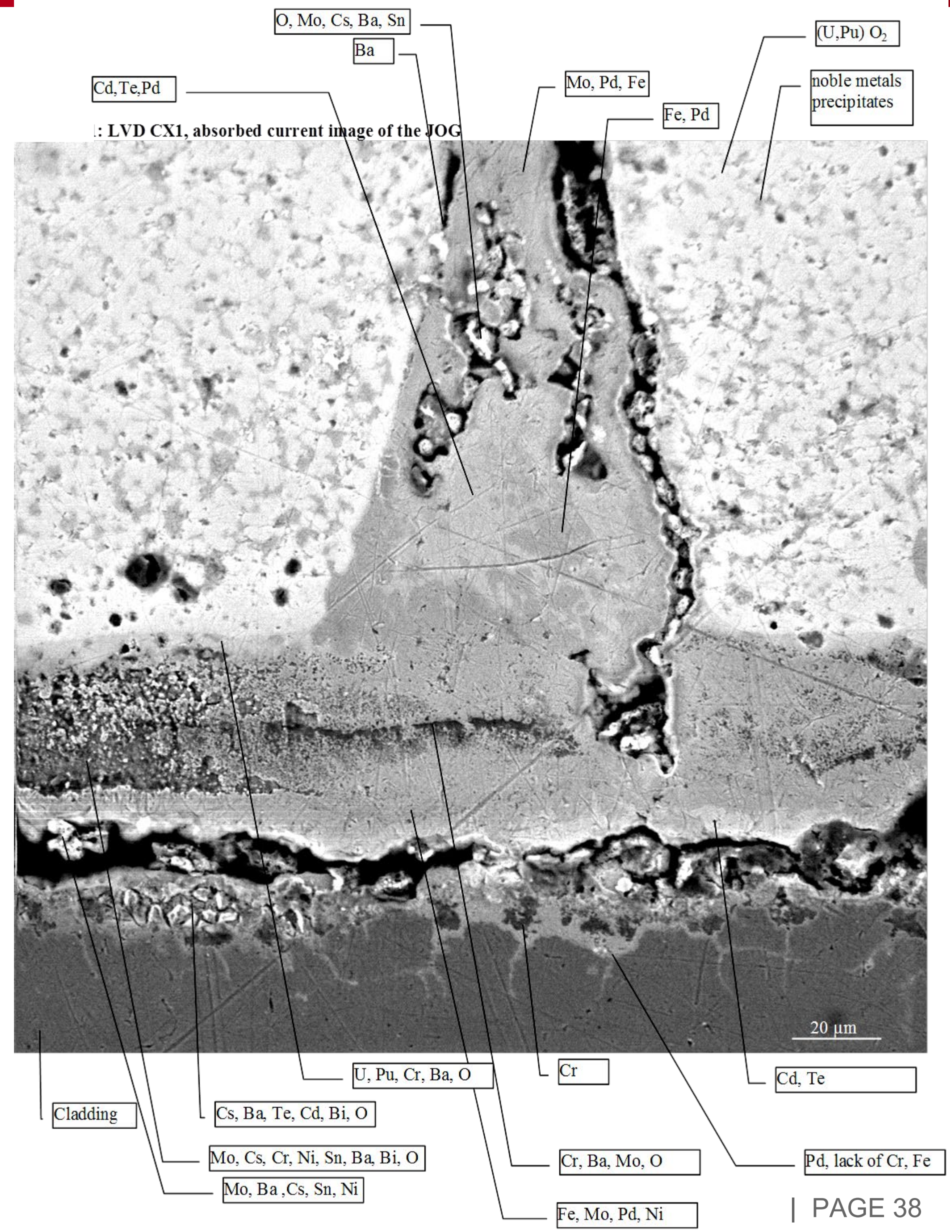

Fission gas local retention measurement

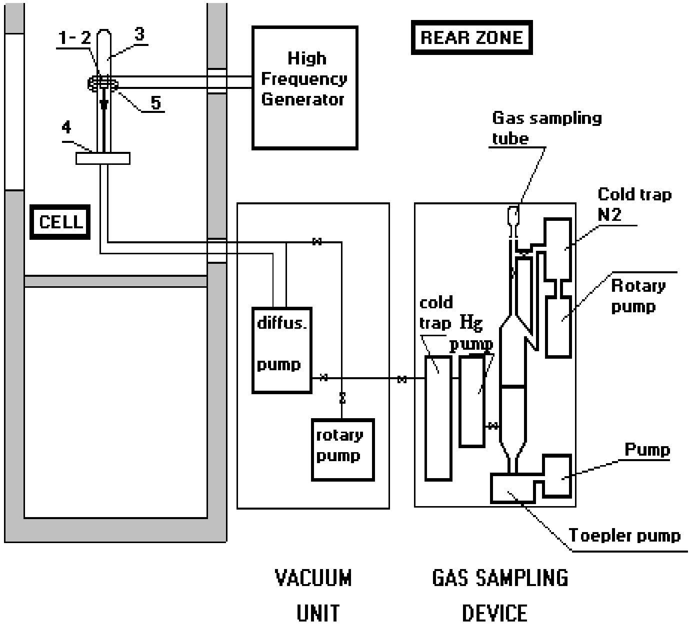

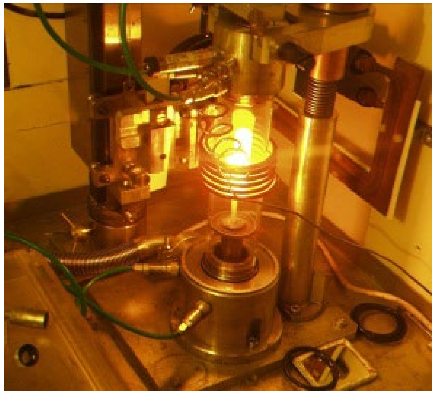

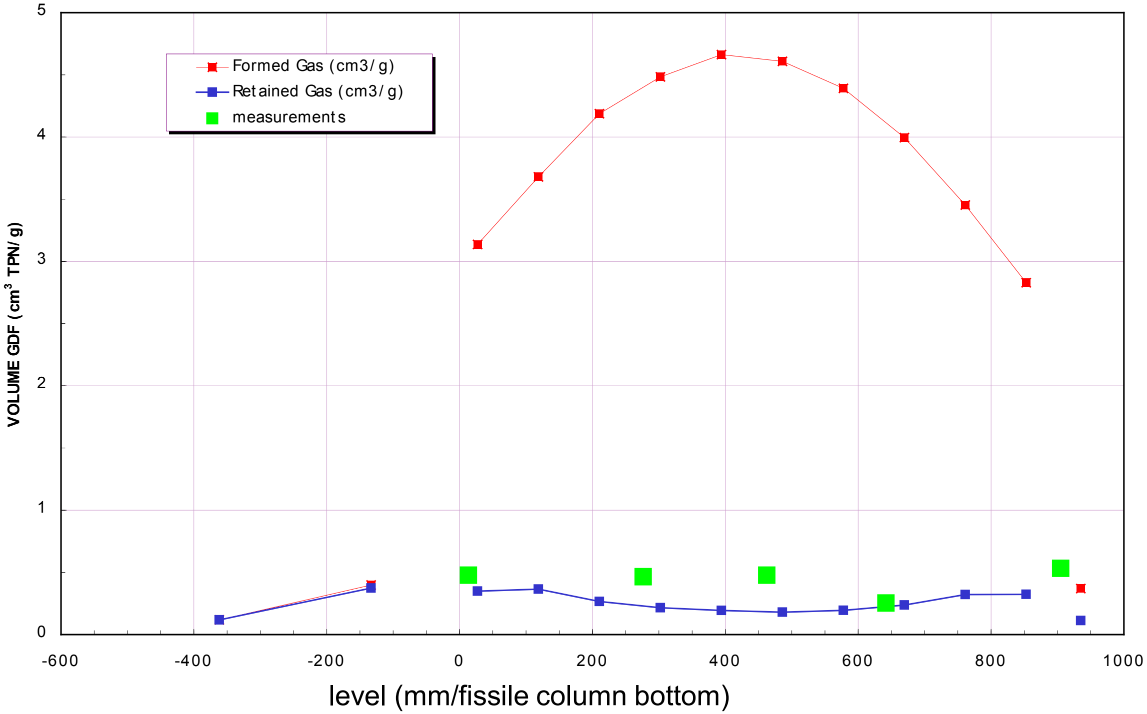

Fission gas local retention measurement

Sublimations

→ drop of occluded gas at ~ 8 at %

≈ same Bu as Mo oxidation and JOG formation

Gas retention in Phénix fuel pins

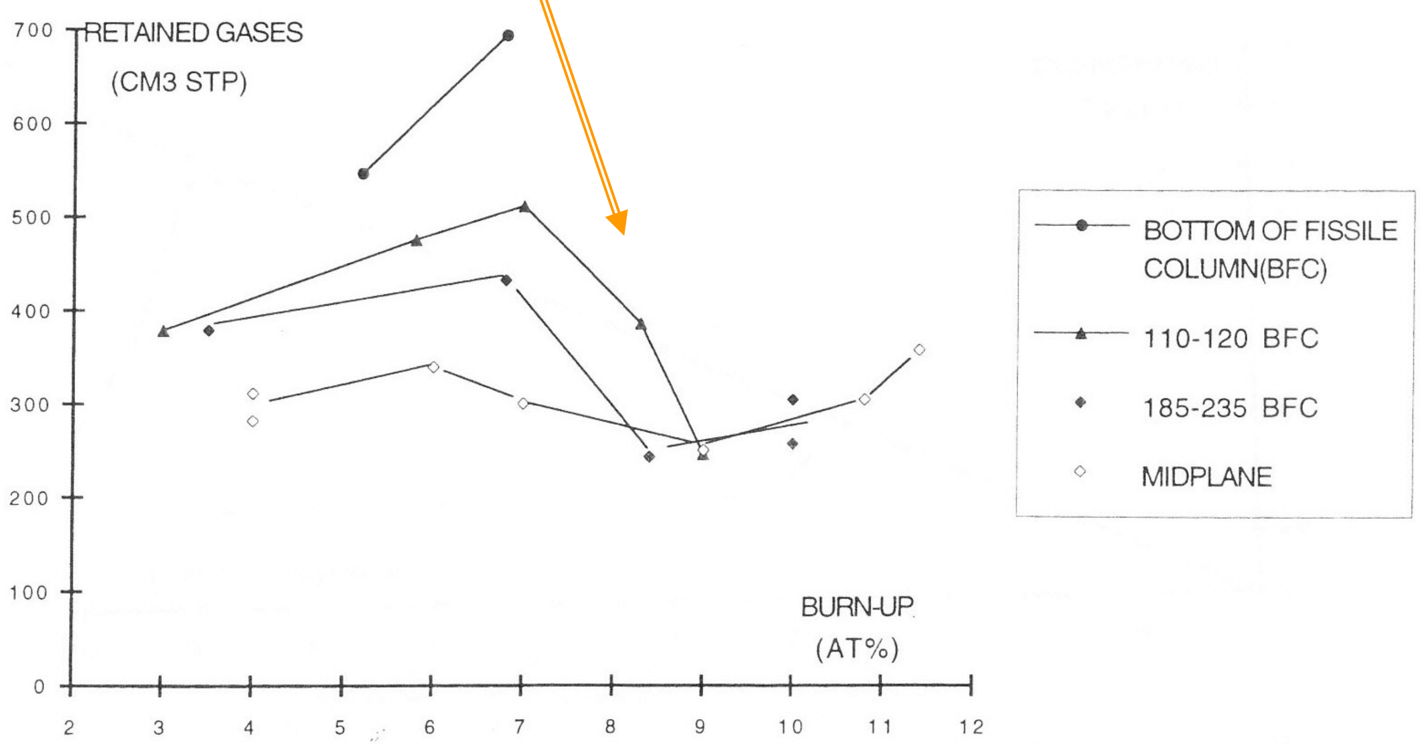

Electron Probe Micro Analyzer / fission gases

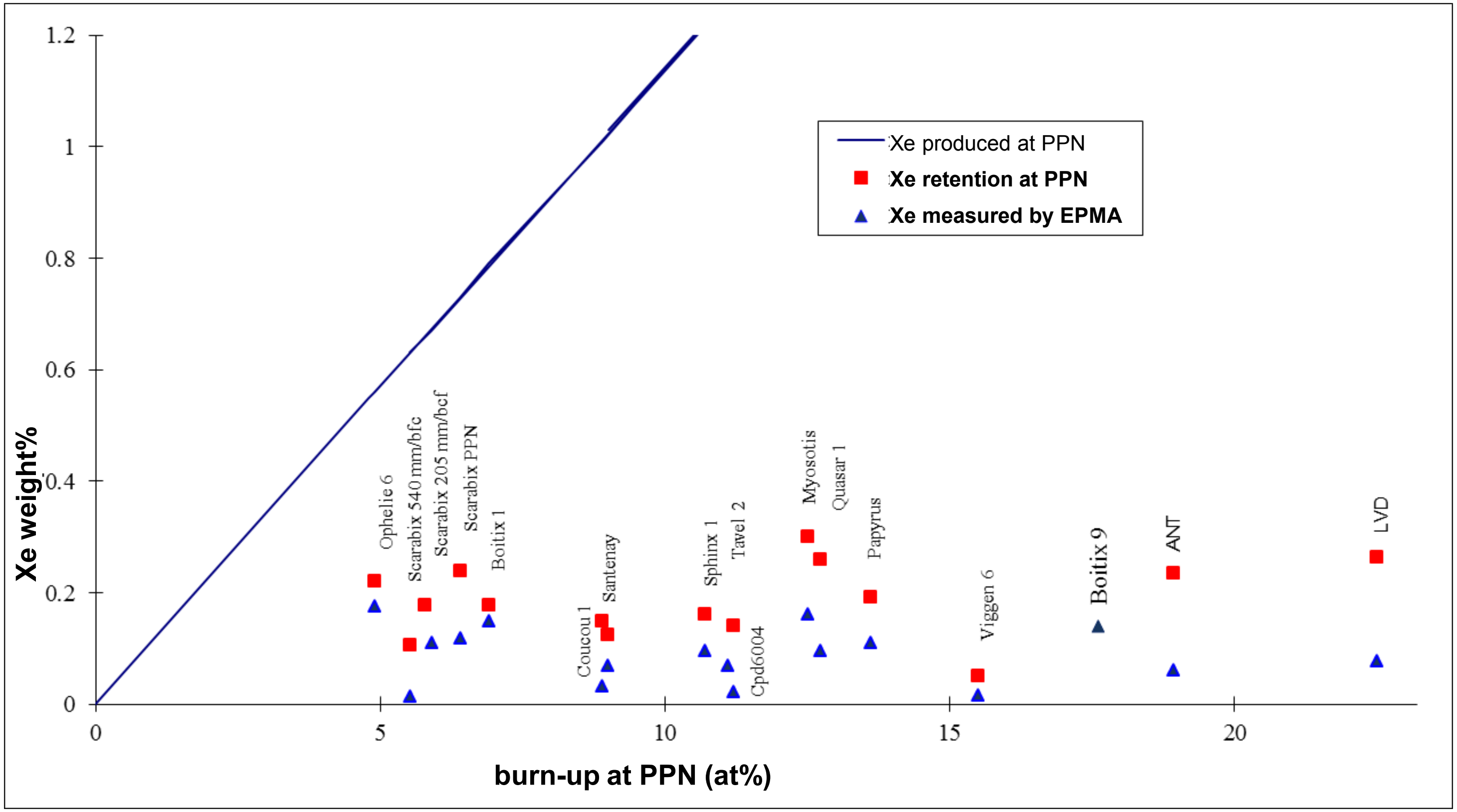

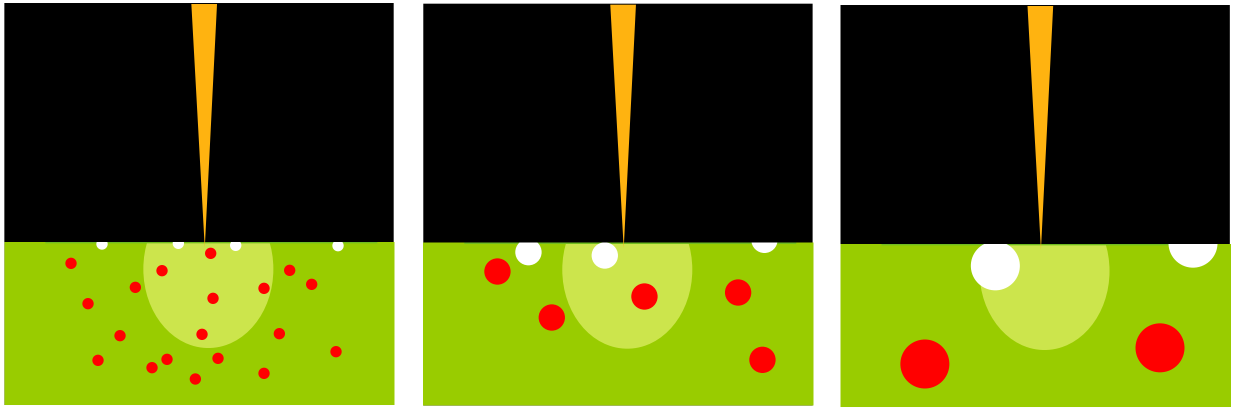

- Because of gas precipitation into bubbles (in addition to high release), EPMA Xe measurement → mainly Xe in the matrix, outside the bubbles.

Electron Probe Micro Analyzer / fission gases

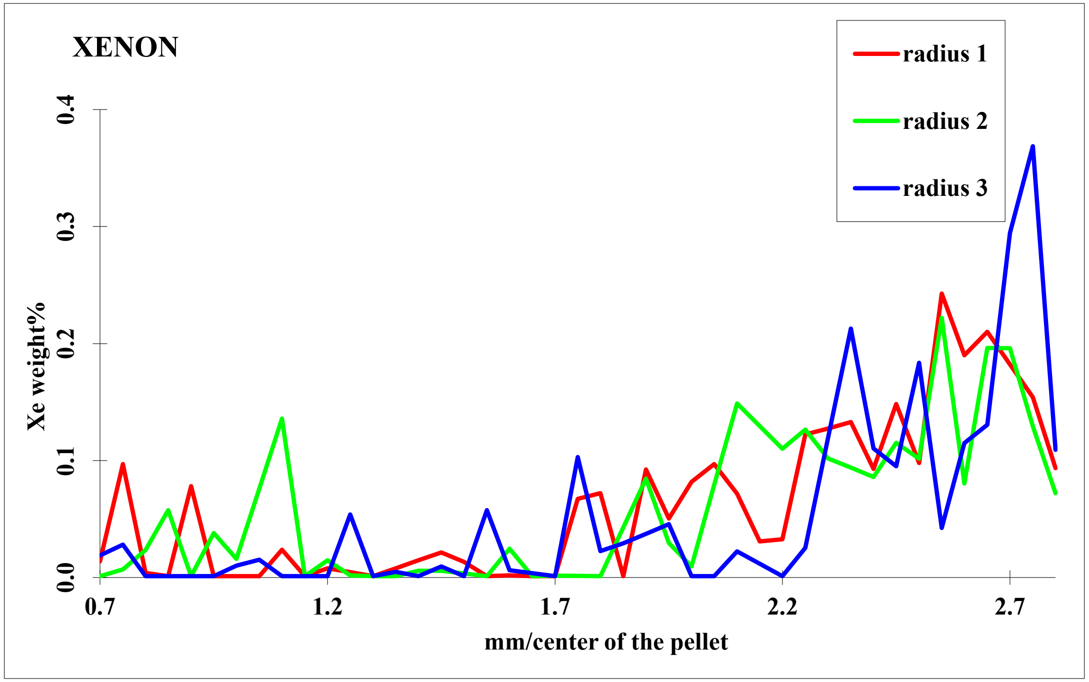

- more gas in the matrix on the periphery than in the center where there is almost no gas

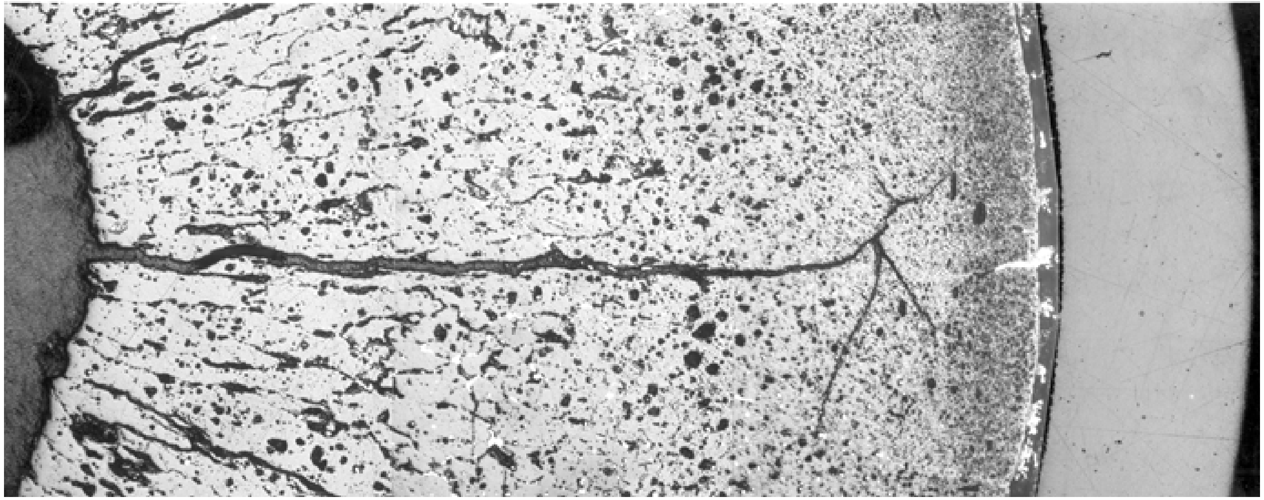

Fission gas release

	pin 126, puncturing	pin 124, gamma ^{85}Kr	pin 125, gamma ^{85}Kr
FGR %	91,2 %	91,1 %	90,4 %

JOG2 test in Cabri (mars 1992)
→ 735 W/cm (PPN)
melt area in the center

	pin 125, after JOG2 puncturing
FGR%	90,9 %

→ very low release during the test, close to the uncertainties

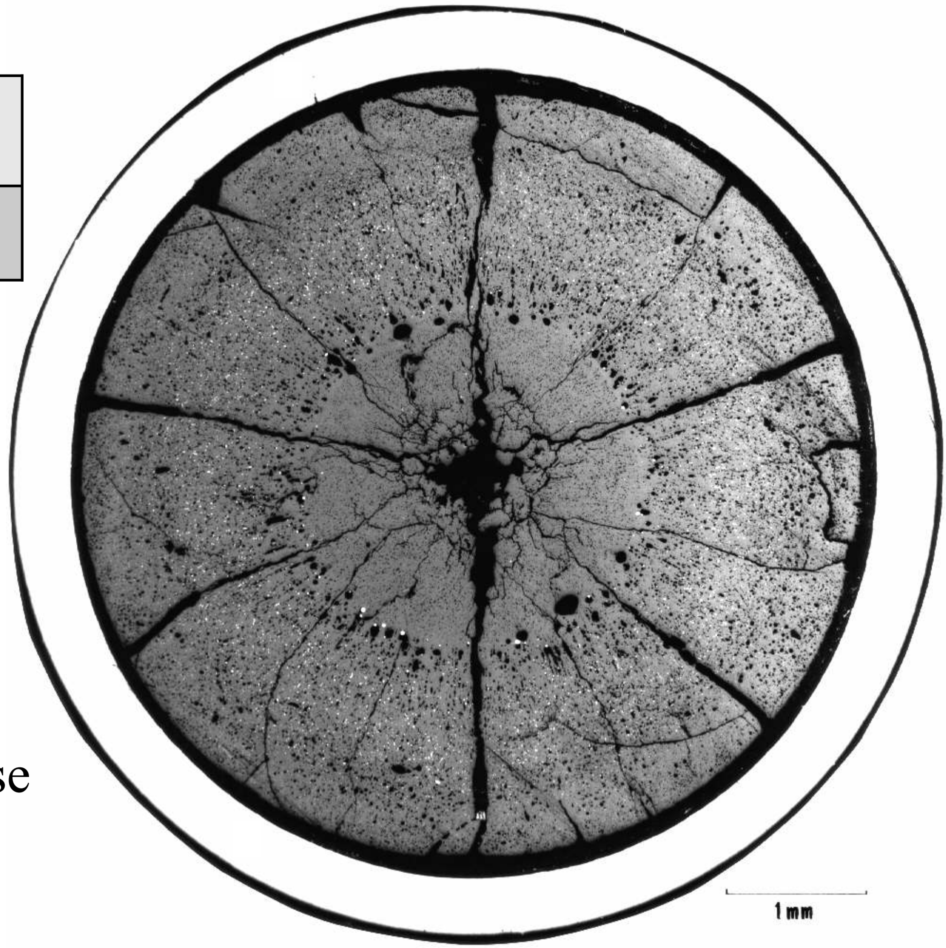

SIMS (secondary ion mass spectrometer)

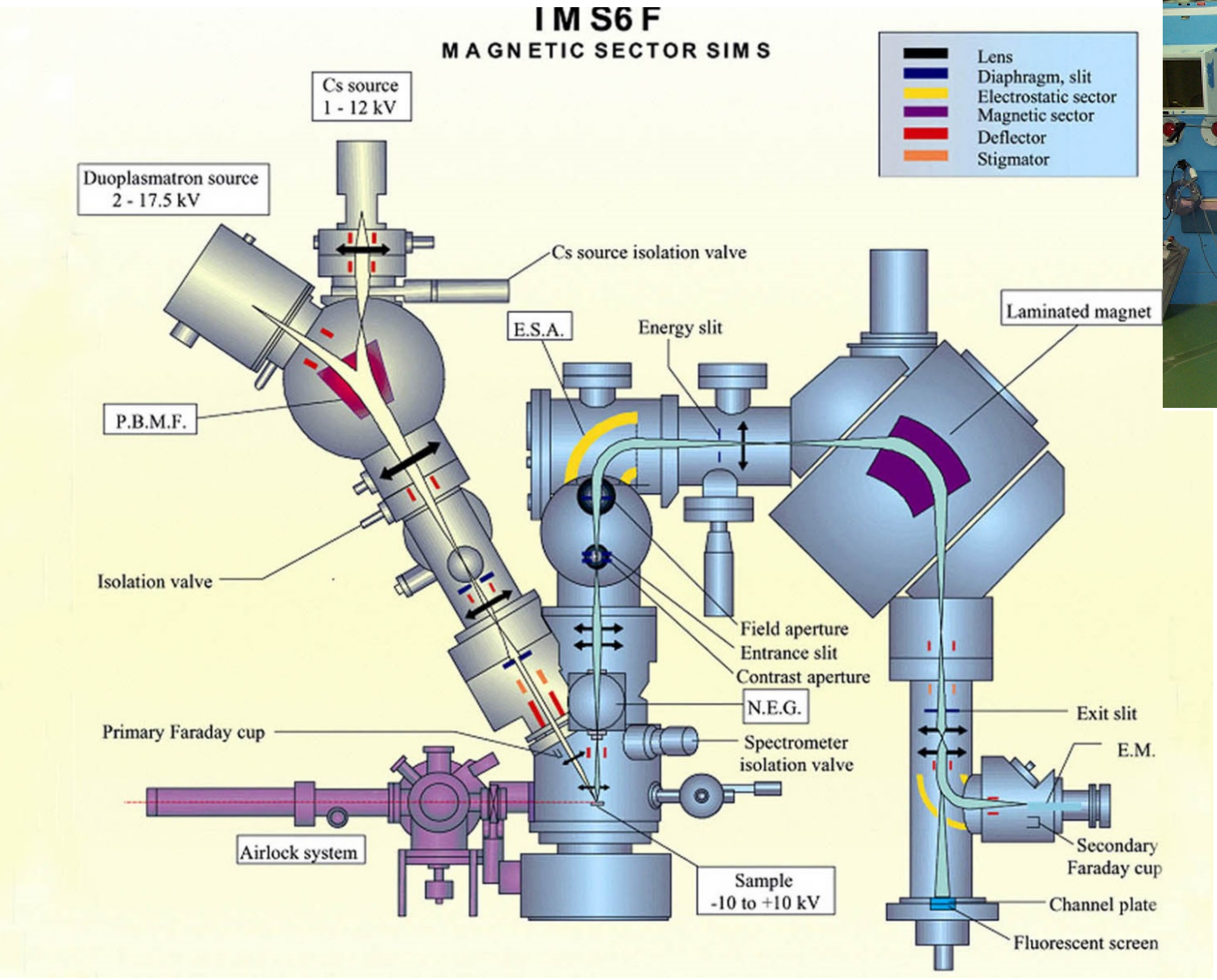

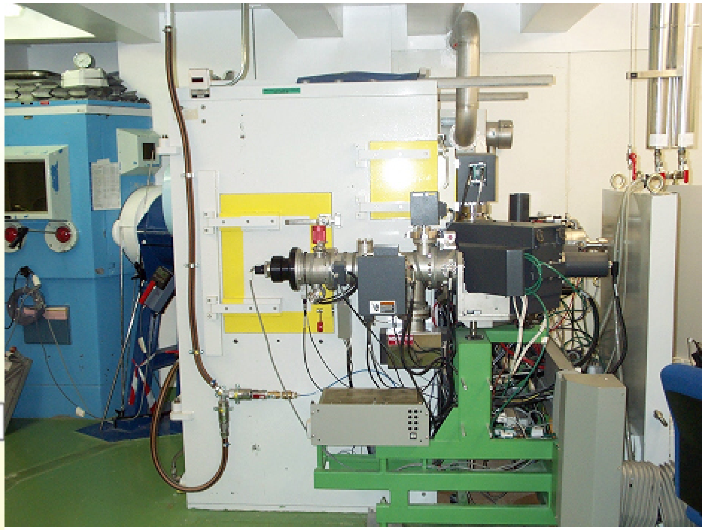

SIMS

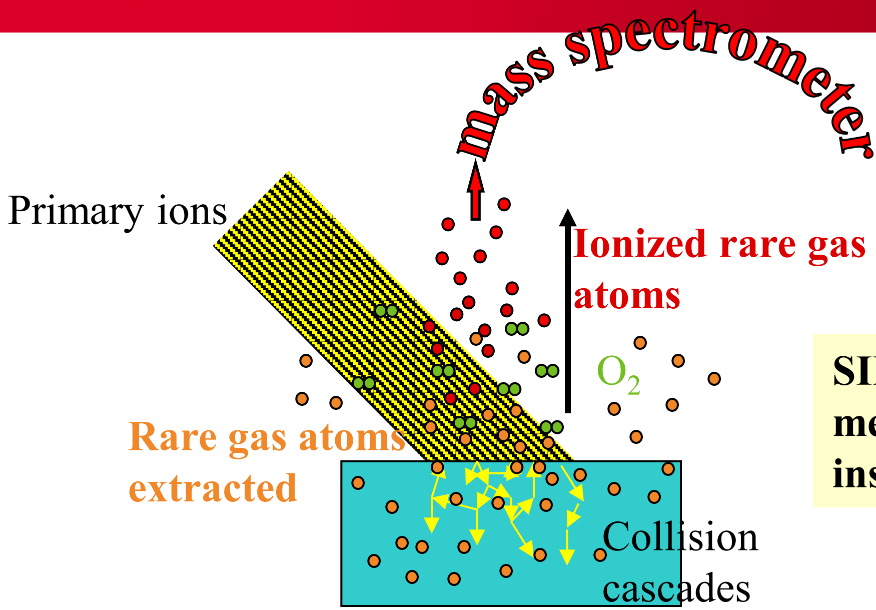

SIMS allows to measure gas content inside bubbles

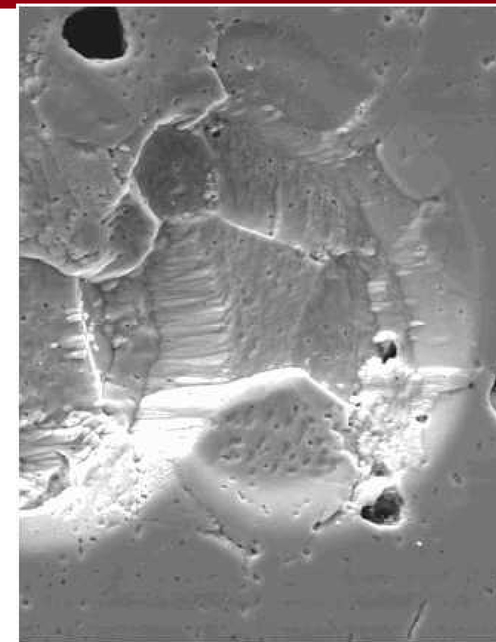

Plasma ionisation above the sample

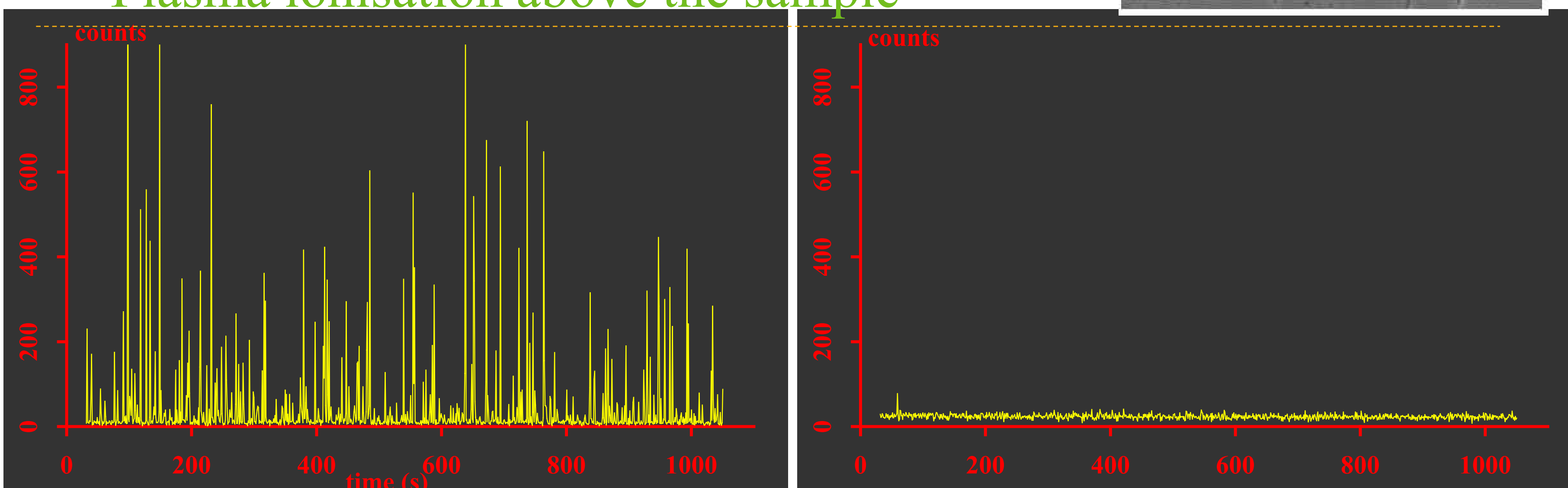

SIMS

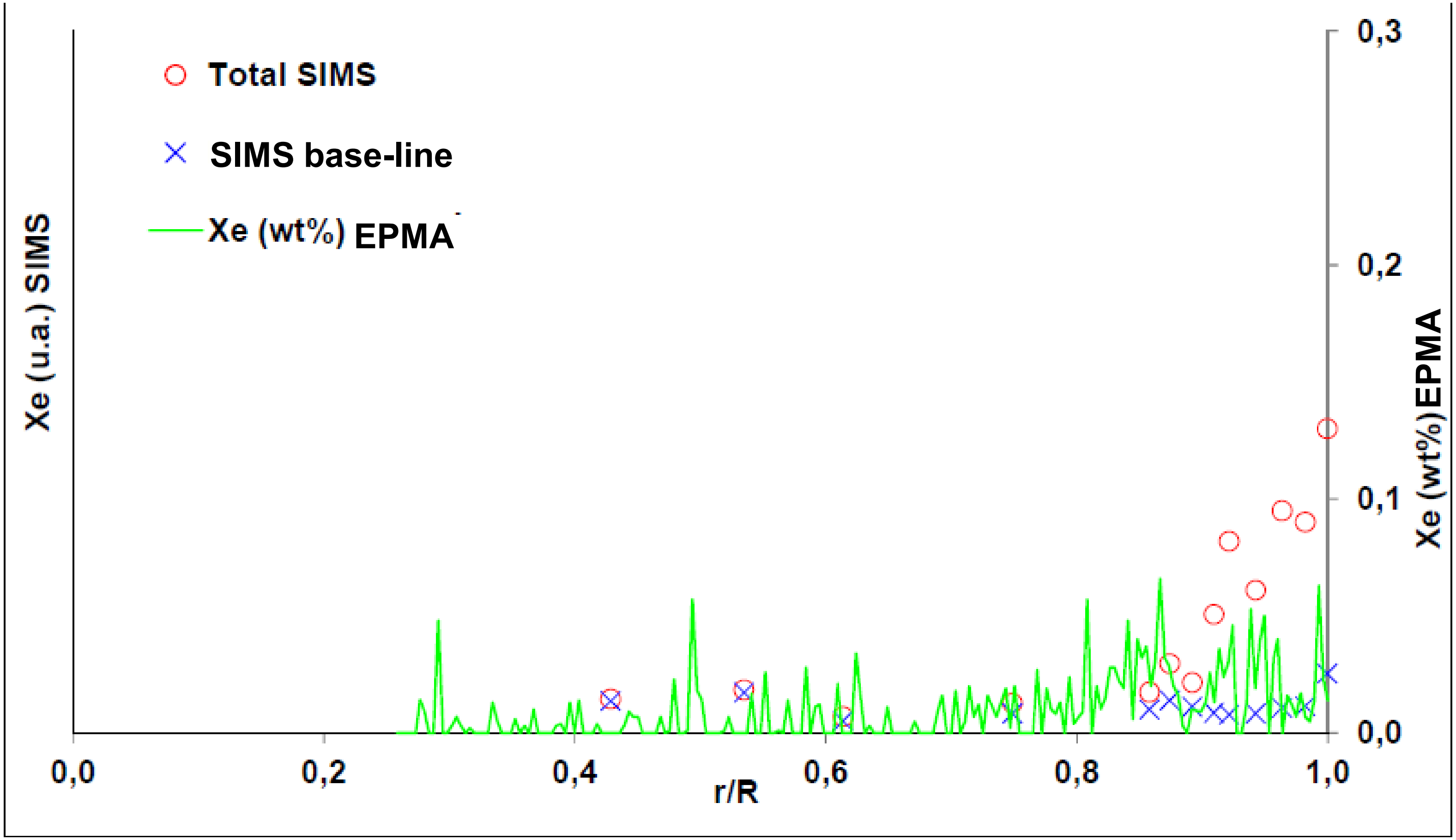

+ ion isotopic images
+ isotopic measurements
+ measurements of light elements

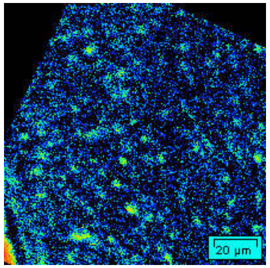

^{129}I map on a fuel periphery

FIB/SEM + EBSD

FIB/SEM (Focused Ion Beam/ Scanning Electron Microscope)

FIB/SEM examination + EBSD (Electron Back-Scattering Diffraction)

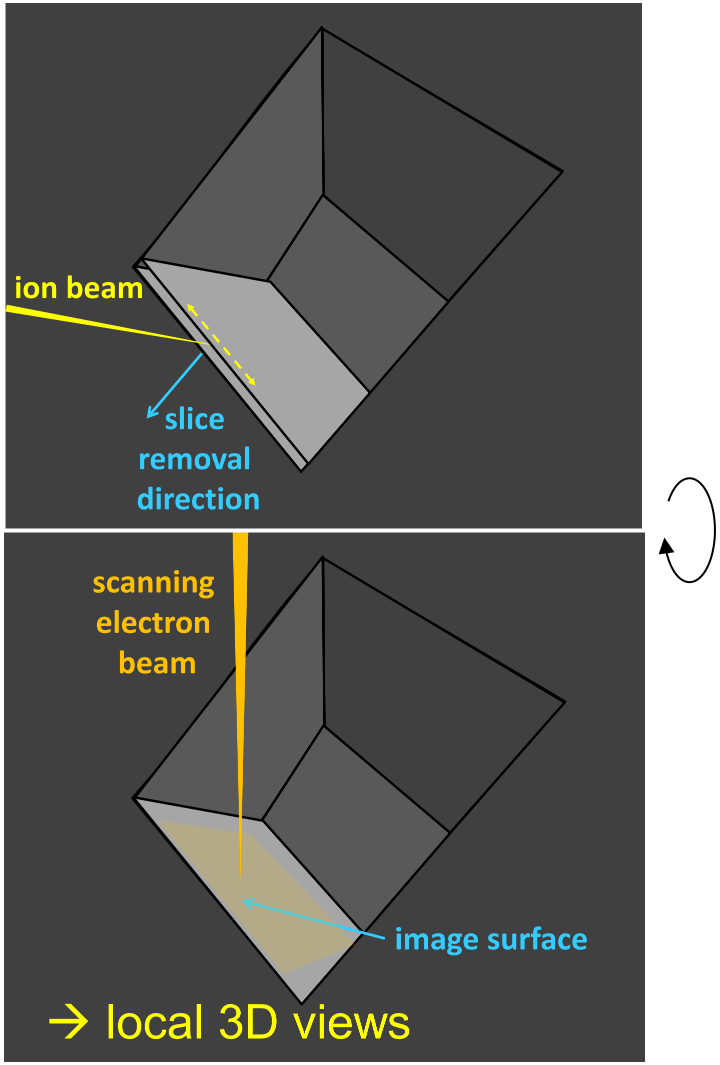

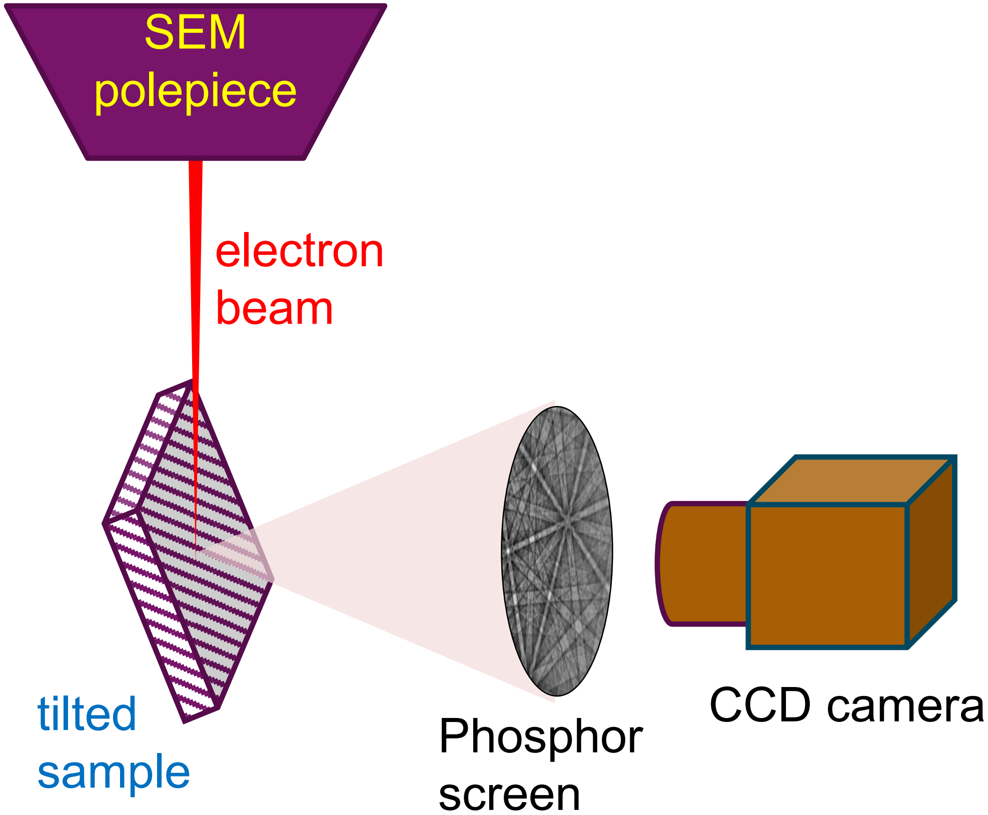

→ grain orientation maps

EBSD example in a PWR fuel

- Initial grains → micrometric domains with small but clear orientation differences

SEM EBSD
Section burn-up
73 GWd/t_U

0.36R

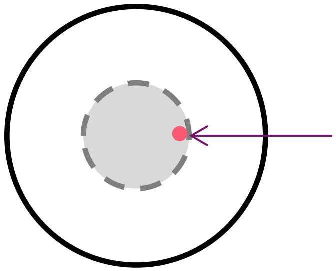

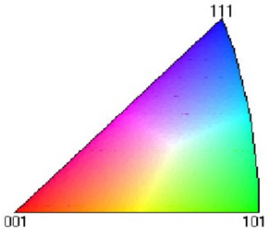

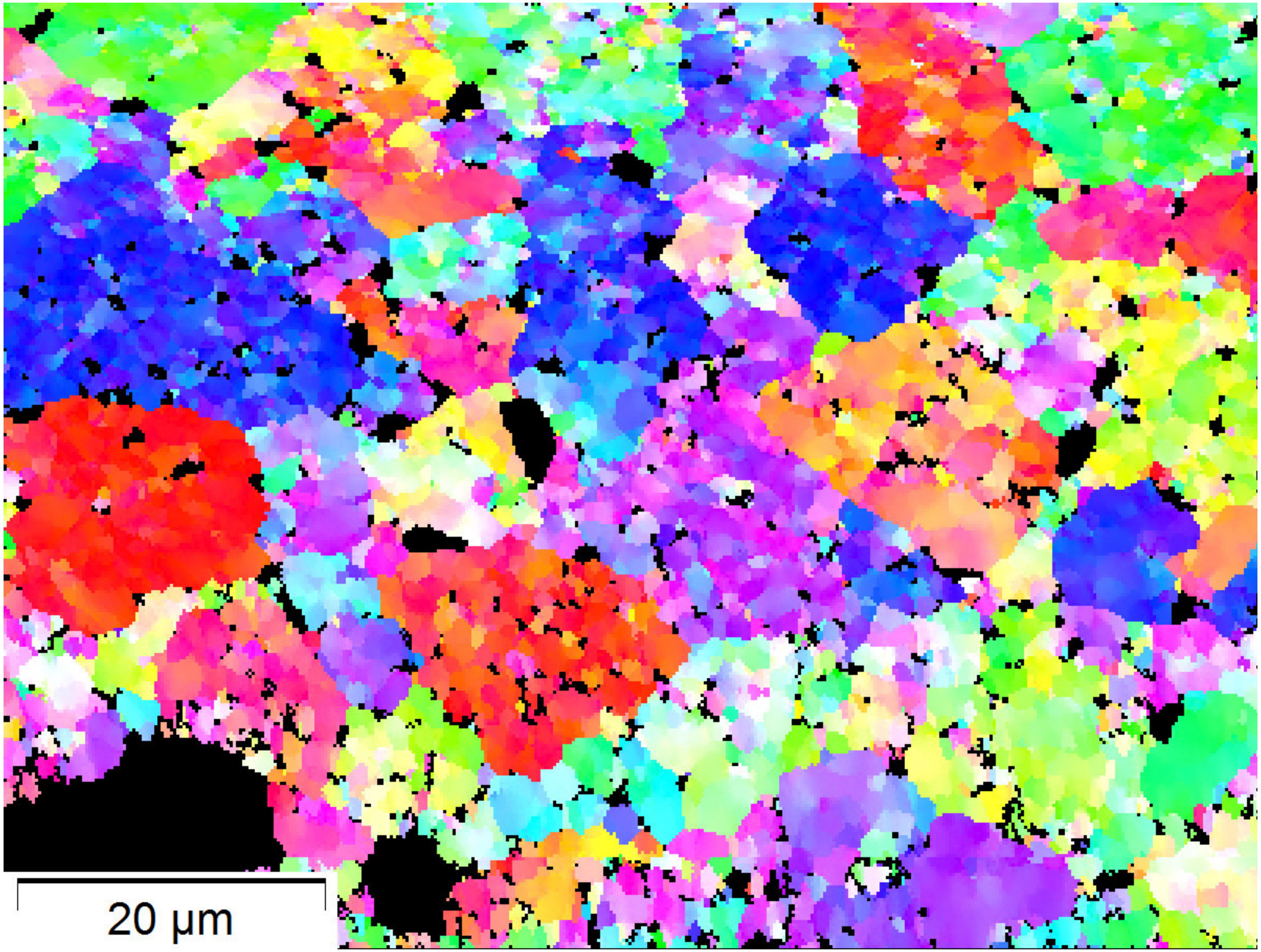

(Noirot NET 2018)

FIB/SEM example in a PWR fuel

- The bubbles initially considered as intra-granular bubbles are actually along the boundaries between these domains
- No interconnected bubble network

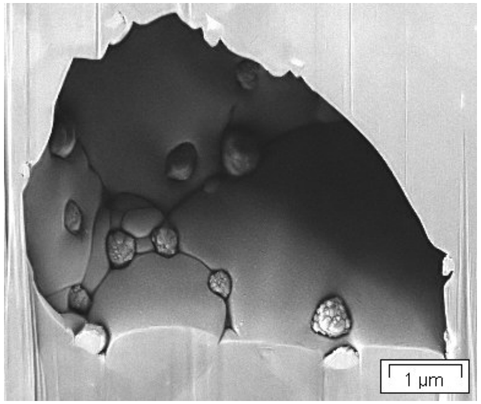

FIB/SEM
Section burn-up
73 GWd/t_U

Center of the pellet 270 images
$26 \times 10 \times 4.6\ \mu m^3$

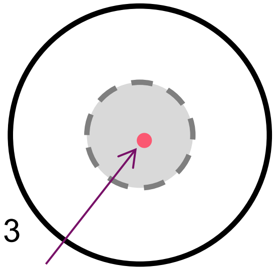

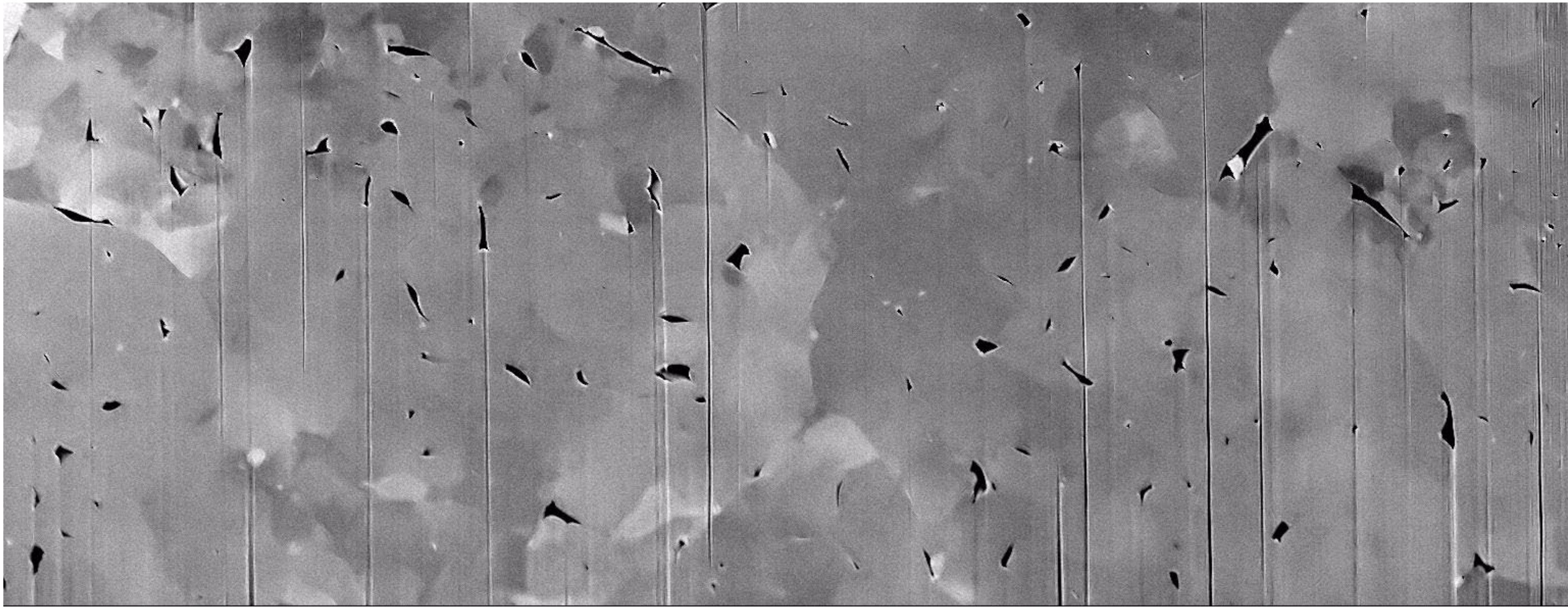

(Noirot NET 2018)

FIB/SEM example in a PWR fuel

- **The shape of the largest of these bubbles can be quite complicated and imply more than two domains, yet they are not interconnected**

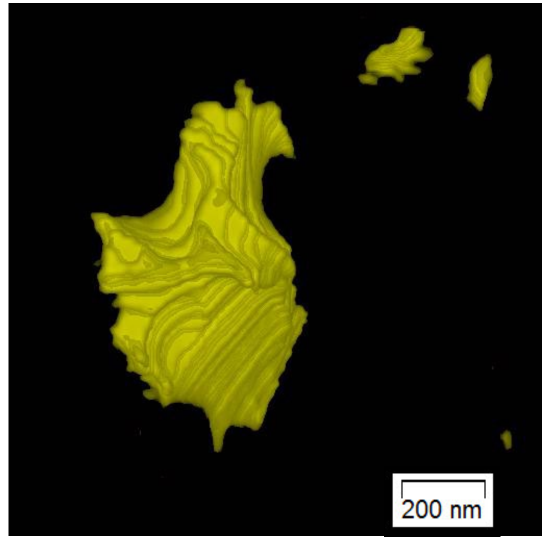

ECD
0.47 µm

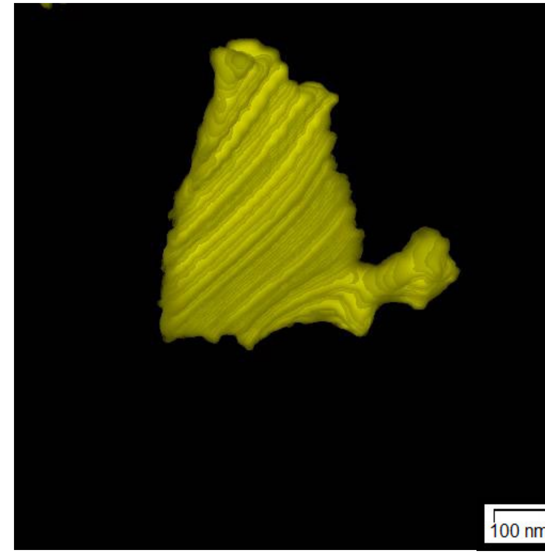

ECD
0.33 µm

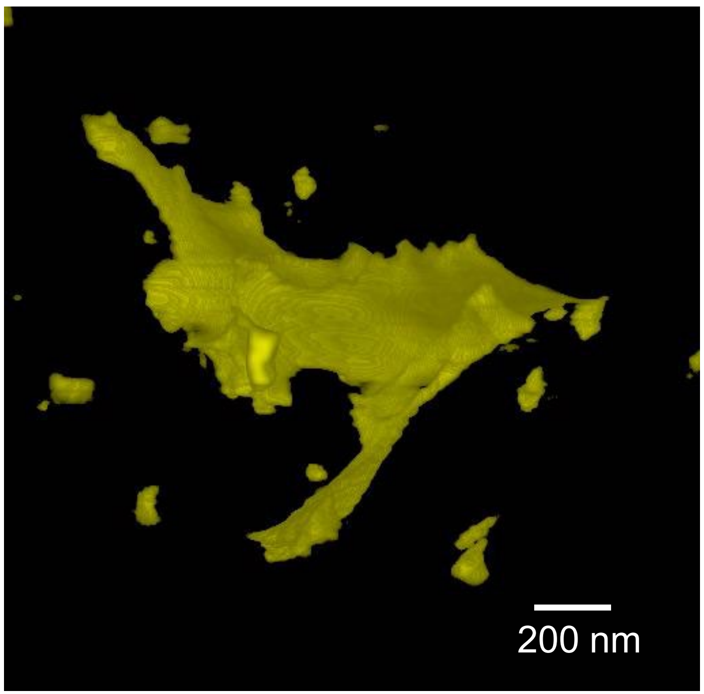

Large bubble ECD
0.61 µm

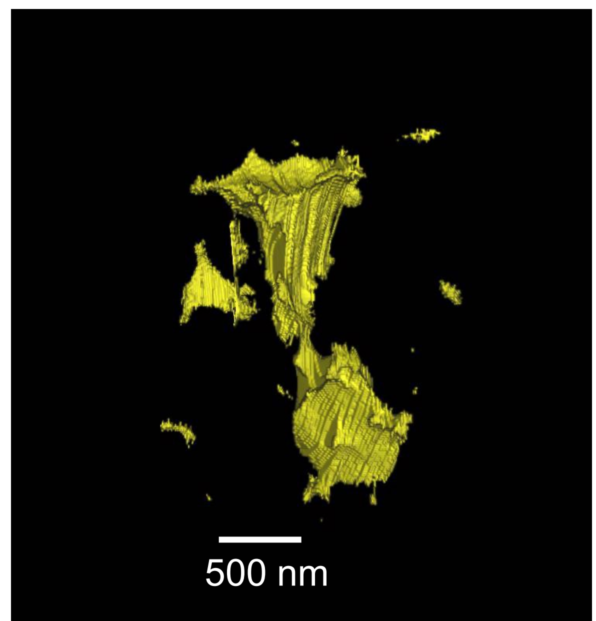

ECD
0.9 µm

(Noirot NET 2018)

FIB/SEM Section burn-up 73 GWd/t_U

INL FIB/SEM + EBSD + EDS on fast reactor fuel

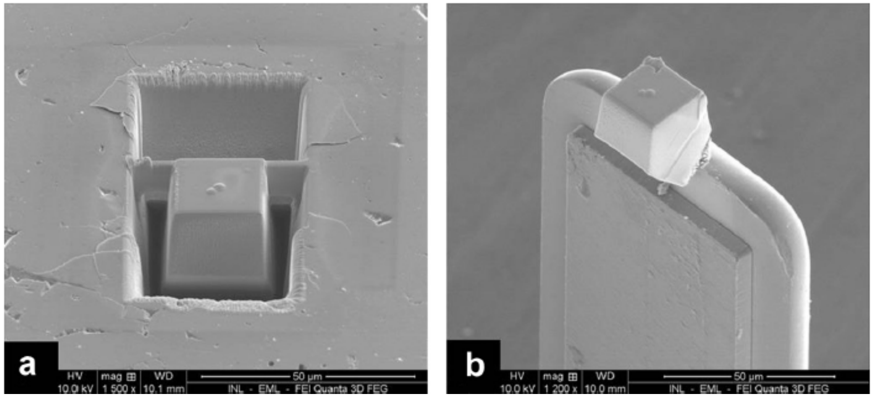

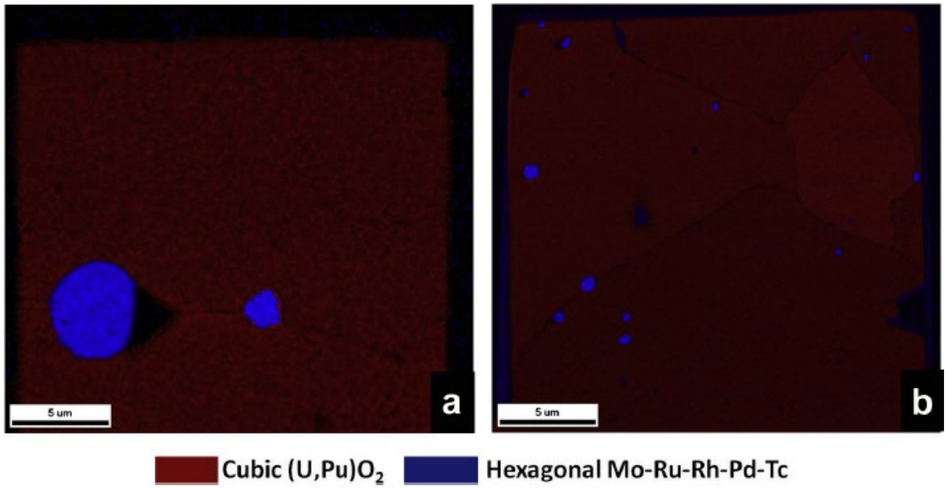

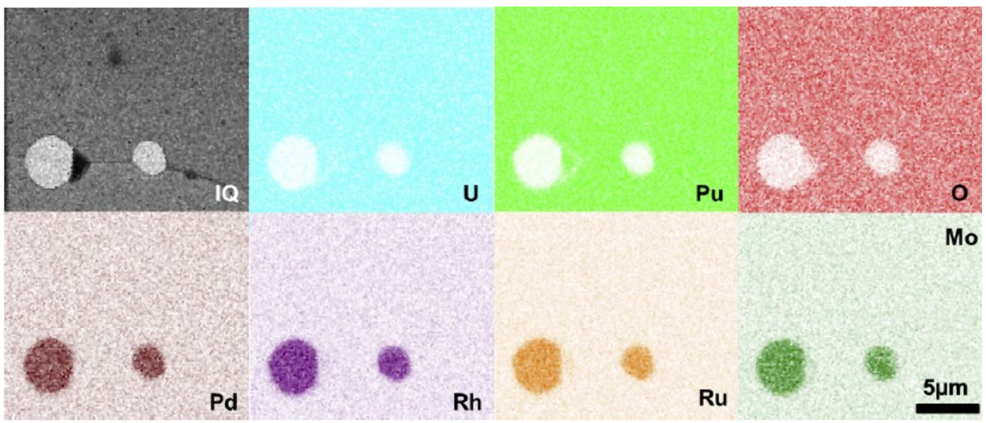

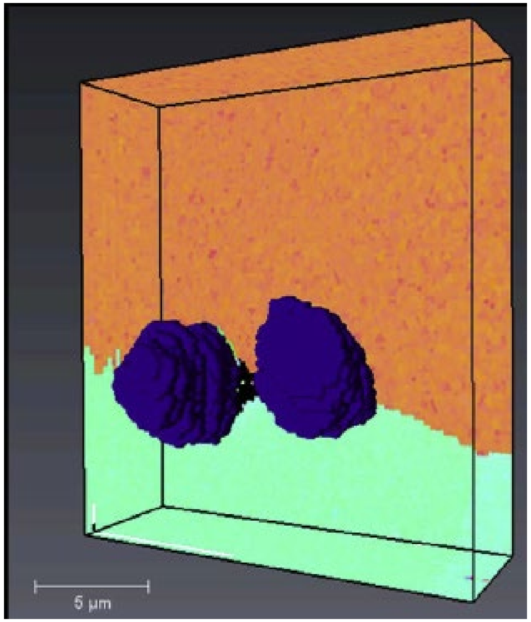

M. Teague et al. JNM 2014

- Only a quick glance at FBR fuel behavior
- Not all PIE techniques were covered (neutron radiography, density measurements, laser ablation, X-ray diffraction, TEM, micro and nano indentation, X-ray fluorescence, various heat treatments including intergranular gas measurements and Knudsen cell tests, burst tests of fuel sections, raman microscopy, dissolution tests for reprocessing, all mechanical testing of the cladding materials…)

Thank you for your attention

Commissariat à l'énergie atomique et aux énergies alternatives
Centre de Cadarache | 13108 Saint Paul lez Durance Cedex
T. +33 (0)4 42 25 44 97 | F. +33 (0)4 42 25 36 11

DEN
DEC
SA3E